AN ABSTRACT OF THE DISSERTATION OF

Emily Townsend for the degree of Doctor of Philosophy in Physics presented on October 11, 2005.

Title: Heavy Fermion Effective Mass in the Superconducting Vortex State

Abstract approved: _____

Allen L. Wasserman

The extended-Lifshitz-Kosevitch formalism (ELK) unifies the treatment of the de Haas-van Alphen (dHvA) effect, allowing it to transcend its traditional roles of mapping Fermi surfaces and measuring effective masses. Here we exploit the capabilities of dHvA as a probe of many-body effects to examine heavy-fermion superconductivity. ELK successfully describes dHvA in heavy fermion materials using a slave-boson model in mean field, and in type-II superconducing materials with the introduction of a self energy due to interactions with the vortex lattice. We propose a model for combining these two many-body effects, and examine its implications for dHvA measurements. The result retains the two important characteristics of its parent models: an enhanced effective mass and temperature-independent damping of the oscillations in the superconducting state. However no suppression of the heavy mass is predicted in the superconducting state, contrary to experiment.

Heavy Fermion Effective Mass in the Superconducting Vortex State

by

Emily Townsend

A DISSERTATION

submitted to

Oregon State University

in partial fulfillment of

the requirements for the

degree of

Doctor of Philosophy

Presented October 11, 2005

Commencement June 2006

Doctor of Philosophy dissertation of Emily Townsend presented on October 11, 2005.

APPROVED:

Major Professor, representing Physics

Chair of the Department of Physics

Dean of the Graduate School

I understand that my dissertation will become part of the permanent collection of Oregon State University libraries. My signature below authorizes release of my dissertation to any reader upon request.

Emily Townsend, Author

ACKNOWLEDGMENTS

All my love and thanks go to the friends and family who have seen me through this process.

Special thanks go to my committee, role models for my professional self since its very inception, and reliable and knowledgeable guides thoughout the journey.

To Allen Wasserman go my admiration, fondness and appreciation, for sharing with me knowledge and deep understanding of the physical universe, genuine trust and friendship, and the recipe for bagels.

My eternal gratitude goes to Corinne Manogue, who by some magnificent wisdom, dedication and kindness, helped me start finishing my thesis when I had completely stalled.

TABLE OF CONTENTS

Page

1 INTRODUCTION 1

2 HEAVY FERMIONS 3

2.1 Properties of the Heavy-Fermion Materials 3

2.2 Origin of behavior: Kondo Impurity and Kondo Lattice Models 3

2.3 Theoretical Methods for Modeling Heavy Fermions 8

2.3.1 The Anderson Impurity Hamiltonian 8

2.3.2 Hubbard X-operators 11

2.3.3 Slave Bosons 11

2.3.4 The Slave-Boson Anderson Lattice Model 13

2.3.5 Green's Matrix 15

3 SUPERCONDUCTIVITY AND THE VORTEX STATE 19

3.1 Properties of Superconductors 19

3.2 Type-II Superconductors and the Vortex State 20

3.3 Unconventional Superconductors 22

3.3.1 Determining the Symmetry of the Order Parameter 24

3.3.2 The Order Parameter of Heavy-Fermion Superconductors 26

3.4 Calculation of the Green's Function in the Vortex State 31

3.4.1 The Effect of a Magnetic Field 32

3.4.2 The Gorkov Equations for a Superconductor 34

3.4.3 The Superconducting Self-Energy in the Vortex State 43

TABLE OF CONTENTS (Continued)

Page

4 THE GREEN'S MATRIX FOR A HEAVY FERMION SUPERCONDUCTOR 46

4.1 Superconducting Self Energy in the Green's Matrix 46

5 DE HAAS-VAN ALPHEN AND THE EXTENDED LIFSHITZ-KOSEVICH METHOD 49

5.1 A Qualitative Explanation of the de Haas-van Alphen Effect 49

5.2 Extended Lifshitz-Kosevitch 53

5.3 Previous Results Using the Extended Lifshitz-Kosevitch Method 54

6 RESULTS 56

6.1 Calculation of m* from the HFSC Green's Matrix 56

6.2 Results: Effective Mass, Amplitude Reduction 64

6.3 Comparison to Experiment 65

7 CONCLUSION 72

BIBLIOGRAPHY 73

7.1 REFERENCES 73

LIST OF FIGURES

Figure		Page
2.1	Renormalized band structure of heavy quasiparticles	8
3.1	Superconducting phases of UPt_3	28
5.1	Landau levels for electrons inside the Fermi surface	50
6.1	Contour of integration	61
6.2	de Haas-van Alphen oscillations for UPd_2Al_3.	67
6.3	de Haas-van Alphen oscillations for $CeRu_2$	67
6.4	de Haas-van Alphen oscillations for URu_2Si_2	68
6.5	Dingle temperature vs. field for UPd_2Al_3	69
6.6	Dingle temperature vs. field for $CeRu_2$	69
6.7	Dingle temperature vs. field for URu_2Si_2	70
6.8	Effective mass vs. field for UPd_2Al_3	70
6.9	Effective mass vs. field for $CeRu_2$	71
6.10	Effective mass vs. field for URu_2Si_2	71

DEDICATION

This document is dedicated to:

My mother, whose immeasurable assistance, love and support have made this accomplishment possible.

My father, who inspired my love of science from the earliest age and has since encouraged my every endeavor wholeheartedly and with love.

My daughter, my joy, who makes every moment of my existence worthwhile.

HEAVY FERMION EFFECTIVE MASS IN THE SUPERCONDUCTING VORTEX STATE

1. INTRODUCTION

Some large percent of what we can observe in solids may be explained within the single-electron model. In this approximation, each electron is treated individually, its interactions with its fellows treated as a simple potential.

The field of strongly-correlated electron systems deals with materials in which this approximation does not apply: The interactions between electrons are crucial for some aspect of the materials' behavior. Two of the most common examples are the topics of this thesis: heavy-fermion materials and superconductors. Chapters 2 and 3 discuss these materials and the models used to describe them.

Chapter 4 presents a model which attempts to describe a material in which both these effects, heaviness and superconductivity, coexist and interact with each other.

De Haas-van Alphen oscillations, or quantum-magneto oscillations, are oscillations in the magnetization of a material as the applied magnetic field is changed. Quantitative analysis of these oscillations reveals not only the shape of the Fermi surface and effective mass of the electrons, but can also give clues to the many-body interactions which are crucial to the behavior of strongly correlated electron systems. Chapter 5 discusses this experiment, and the consequences of these interactions in this experiment.

Chapter 6 examines the model of chapter 4 in the light of the de Haas-van Alphen experiment, and makes comparisons to actual experimental results. This is followed by a short conclusion.

2. HEAVY FERMIONS

2.1. Properties of the Heavy-Fermion Materials

Heavy fermion materials are alloys that show Fermi-liquid behavior at low temperatures but with highly enhanced effective mass. They were first observed by Andres et al [1] in 1975 in $CeAl_3$. The mass enhancement is seen in properties such as paramagnetic susceptibility, heat capacity, resistivity and de Haas-van Alphen, all of which depend on the electron effective mass.

Although at room temperatures Curie-Weiss paramagnetism for strong local moments is observed [2], the zero temperature ground state of the heavy-fermions may be normal (paramagnetic), superconducting, or antiferromagnetic. The antiferromagnetic order may occur with very weak effective moments, orders of magnitude smaller than the Curie-Weiss moments. The superconducting state may emerge out of the antiferromagnetic state, or even coexist with it, in contrast to more traditional superconductors.

Some heavy-fermion materials are listed in table 2.1, along with some relevant parameters (linear specific heat coefficient, γ; superconducting transition temperature, T_c; Néel antiferromagnetic ordering temperature, T_N; magnetic moment of the antiferromagnetic order, μ_{AF}; and Curie-Weiss itinerant magnetic moment, μ_{CW}. In typical, non-heavy metals γ is in the range of 0.7 - 5 mJ/mol K^2 [3]

2.2. Origin of behavior: Kondo Impurity and Kondo Lattice Models

The heavy-fermion compounds contain a sublattice of rare earths such as cerium or uranium, or occasionally, ytterbium or samarium, each of which has a local magnetic moment. This is embedded in an ordinary Fermi sea provided by such

Material	γ (mJ/mol K^2)	T_c	T_N	μ_{AF}	μ_{CW}
$CeCoIn_5$	290-1000 [4]	2.3K [4]	none	none	$2.59\mu_B$ [4]
$CeRu_2$	27 - 29 [5], [6]	6.1 K [7]	45 K [8]	$10^{-4}\mu_B$ [8]	$0.27 - 0.6\mu_B$ [8]
UPd_2Al_3	150 [9]	2K [9]	14.5 [9]	$0.85\mu_B$ [10]	$3.4\mu_B$ [11]
URu_2Si_2	75 [12] - 180 [13]	1.4 K [14]	17.5 K [12]	$0.03\mu_B$ [13]	$3.51\mu_B$ [13]
$CeAl_3$	1620 [1]	none	none	none	$2.63\mu_B$ [1]

TABLE 2.1. Some heavy fermion materials

elements as aluminum, copper, silicon, zinc, cadmium, platinum, gold, beryllium, ruthenium, or indium. The rare earths have their valence electrons in unfilled f-shell states, which are highly localized. This localization provides a strong repulsive Coulomb interaction (U) for any additional electrons occupying the same site [15]. This is referred to as the on-site correlation.

In the cerium alloys the f states are singly occupied, lying below the Fermi energy at ϵ_f, while the effective energy of a second electron occupying that state, $\epsilon_f + U$, lies well above the Fermi energy. The single f electron is a localized magnetic moment. So the model we consider is a regular lattice of localized spins at the sites of the rare earth atoms and a Fermi sea of itinerant states. The two kinds of states are mixed, essentially by band structure.

The combination of strong on-site correlation and hybridization between localized unpaired electrons and the Fermi sea is known as the Kondo problem. It is relevant to materials with dilute magnetic impurities, and its signature is a minimum in resistivity. With decreasing temperature, resistivity decreases according to a power law, as expected for phonon scattering. But below a temperature in the

range of 3 - 40 Kelvin, the Kondo temperature, the resistivity begins to increase with cooling, ultimately appraoching the limit for non-magnetic impurities.

If we neglect either the strong on-site correlations or the hybridization of the conduction and localized electrons either remaining piece of the problem is tractable. But the situation at hand is the more complex problem of a local moment interacting with conduction electrons.

First, let us consider the case without hybridization. The addition of angular momentum for two spin one-half particles (such as the localized f electron and a conduction electron) yields two kinds of states: a spin singlet state with net spin of zero and a three-fold degenerate spin triplet state, with net spin of one. In our case the non-degenerate spin singlet is the lower energy state. (Because of this, the system can be modeled using an antiferromagnetic interaction between a local moment and conduction electrons.) In this state (well below the Kondo temperature), the local moment is quenched or screened (net spin of zero). This spin singlet is a many-body effect, that is, it arises from the quantum statistics of multiple identical particles.

If, on the other hand, we neglect the correlations and consider the hybridization of the conduction electrons with the localized state, we have essentially a single-electron problem. In other words, we have a diagonalizable Hamiltonian, which simply has new eigenvalues, but retains a description in terms of single electrons. The result in this case is a virtual-bound-state resonance. The resonance is a peak in the density of states at an energy that is slightly higher than the energy of an electron that is actually occupying the localized state. This is analogous to a virtual bound state in a solid, with a peak in the conduction band density of states. If that peak occurs near or right at the Fermi energy, the effective mass looks large, i.e. the specific heat and zero-field paramagnetic susceptibility are enhanced ([16] p 73, [17] p 936, [2] p 9). This is a single-particle effect. It does yield an enhancement in

the density of states, however without the correlations or magnetic interactions we do not see the Kondo temperature minimum or Curie behavior [2]

The correct description of Kondo impurity materials includes both the hybridization and strong on-site correlations. The models for dealing with both of these features simultaneously, and their extensions to Kondo lattices, will be discussed in the next section. The main feature of these models is a many-body effect called the Kondo or Abrikosov-Suhl resonance. This resonance is once again a peak in the density of states, which occurs at an energy defined by a "Kondo temperature", at or just above the Fermi energy. (This is not the energy of the original localized state.) It is a many-body resonance due to the strong on-site correlation, U, for the f states. However if this correlation is removed ($U \to 0$) the resonance becomes the single-particle resonance of a virtual bound state.([2] p 409) The Kondo resonance is responsible for an enhanced scattering at low temperatures which is the cause of the resistance minimum, as well as an increase in the density of states at the Fermi energy resulting in the low-temperature quenching of the local moments and enhanced values for the zero-field magnetic susceptibility and linear specific heat coefficient. These enhancements reflect the fact that more quasi-particle excitations (final states) are available to the system than in a typical metal, due to the Kondo resonance.

Well below the Kondo temperature, impurity materials display an approximately temperature-independent Pauli susceptibility characteristic of a Fermi liquid, the local moments having been quenched [18] [19]. At temperatures near the Kondo temperature, the susceptibility decreases with temperature squared ([2] p 267, 52), $\chi(T) = A - BT^2$. As the temperature is further increased the local moments begin to appear, as the range of the correlation between the screening conduction electrons and the local moments decreases. In this temperature range the susceptibility

is given by a Curie expression, $\chi \sim \frac{\mu_{eff}^2}{T}$, with the effective moment increasing logarithmically with temperature, $\mu_{eff} \sim \mu_f(1 - \frac{1}{\ln(T/T_K)})$ ([2] p 406) until it eventually reaches the value for the total angular momentum of a singly occupied f site, totally unscreened by the conduction electrons. (The term $\frac{T}{T_K}$ appears because $k_B T_K$ is the energy scale at which perturbation theory breaks down due to the Kondo many-body renormalization.)

The fundamental difference between Kondo impurity systems and heavy-fermion materials is the onset of coherence between the localized impurity sites. The RKKY (Ruderman, Kittel, Kasuya, Yosida) interaction is an indirect exchange interaction between two spins, mediated by conduction electrons, and is responsible for this coherence. A heavy-fermion material has local moments at all the cerium (uranium, et cetera) atoms in the solid, rather than occurring as dispersed, statistically random impurities. (Thus the descriptor "Kondo Lattice" that is sometimes applied to heavy-fermion materials.) The result of coherent, locally correlated f states hybridizing with conduction electrons is a new, renormalized band structure. As seen in figure 2.1, near the Fermi energy the band is very flat, giving an enhanced effective mass ($\frac{1}{m^*} = \frac{dE_k}{dk}$). The enhanced specific heat coefficient of Kondo-lattice materials, when considered as an enhancement per impurity atom, may be comparable to Kondo impurities [19] however the term "heavy-fermion" is generally applied to those materials for which the enhancement is more dramatic [2]. The coherence also changes the low-temperature resistivity for a Kondo lattice, as compared to isolated impurities [18]. Since the lowest temperature scattering is coherent, the resistivity once again decreases as temperature goes to zero. The magnetic susceptibility of heavy-fermion materials displays a Curie to Pauli crossover as in the impurity materials, however at low temperatures the interactions between local mo-

ments allows for the possibility of an ordered (usually antiferromagnetic) ground state. Screening by the conduction electrons (recall the singlet state) is probably responsible for the small size of the moments in the antiferromagnetic order.

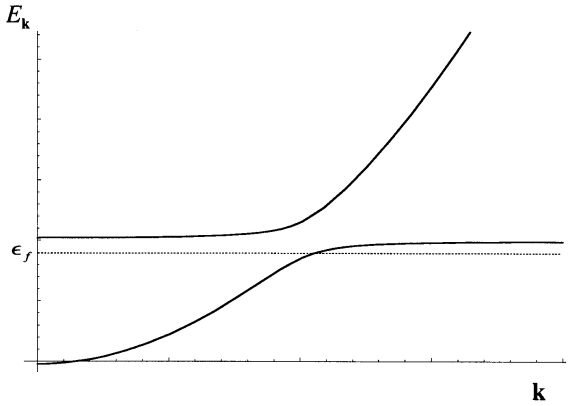

FIGURE 2.1. Renormalized band structure of heavy quasiparticles. The band is flat near the Fermi energy, ϵ_f.

2.3. Theoretical Methods for Modeling Heavy Fermions

2.3.1. The Anderson Impurity Hamiltonian

Models for heavy-fermion materials are largely extensions of models for Kondo impurity materials, and it is useful to begin with this simpler case. A single f-electron state with strong on-site correlation and hybridization with conduction electron states may be described by the Anderson Hamiltonian. [15]

$$H = \sum_{k,m} \mathcal{E}_{\mathbf{k},m} c^\dagger_{\mathbf{k},m} c_{\mathbf{k},m} + \sum_{\mathbf{k},m} (V_{\mathbf{k}} f^\dagger_m c_{\mathbf{k},m} + V^*_{\mathbf{k}} f_m c^\dagger_{\mathbf{k},m}) \qquad (2.1)$$
$$+ \sum_m \left(E_f f^\dagger_m f_m + U f^\dagger_m f_m f^\dagger_{-m} f_{-m} \right).$$

The operator $c^\dagger_{\mathbf{k},m}$ creates a particle in the conduction band, with momentum $\mathbf{k}$ and spin m, while $f^\dagger_m$ creates a particle on the cerium site with spin m. As usual

$c^\dagger_{\mathbf{k},m} c_{\mathbf{k},m}$ counts the number of electrons in the state $|\mathbf{k}, m\rangle$, and $\mathcal{E}_{\mathbf{k},m}$ and E_f are the energies of an electron in the conduction band and on the f site respectively. U is the on site correlation energy, i.e. the interaction energy of two f electrons on the impurity site, necessarily with opposite spins. $V_{\mathbf{k}}$ describes the hybridization potential between the conduction and localized f-electron states.

The site of the impurity is taken as the origin, and angular momentum with respect to this origin is a conserved quantity and a good quantum number. For the localized state this means the designation as an f-electron state, that is a state with angular momentum of $l = 3$, is retained. Therefore this state hybridizes only with those conduction electrons which also have angular momentum $l = 3$. The other states are decoupled from the f-electrons (and all their difficulties), and can be ignored for our purposes.

When this "orbital" angular momentum is combined with spin, every electron in the problem has good total angular momentum, J, which is either $l + s = \frac{7}{2}$ or $l - s = \frac{5}{2}$. Spin-orbit coupling (Hund's rules) dictates that the $J = \frac{5}{2}$ states are the lower in energy, and we have a degeneracy of $N = 2J + 1 = 6$. The "spin" quantum number m in the Anderson Hamiltonian above is more properly m_J and denotes these six states, $-J \leq m_J \leq J$.

(This applies to cerium, which has one electron in the 4f shell. Ytterbium has one hole, so the $J = \frac{7}{2}$ states are lower in energy, and $N = 8$. Thulium has two holes, and uranium three electrons, making them more complicated to describe theoretically.)

A perturbation expansion in U might seem appealing. This would be nice because in the $U \to 0$ limit we have a non-interacting system, which suggests the use of a standard perturbation expansion and Wick's theorem. But in heavy-fermion and Kondo systems U is large, and this strong correlation is the very basis of the

effects. As in superconductivity, we don't get the extraordinary by expanding about the ordinary. In fact, the approximation we'll eventually make is $U \to \infty$. So a small U expansion must be tossed out as irrelevant.

The hybridization parameter, V, on the other hand, is more likely to be small, and is a good candidate for an expansion. Unfortunately for our expansion, the $V \to 0$ limit already has correlations. While this very feature commends it for describing these effects, it means the many-body states of this problem are created by operators with non-standard commutation relations, which prevent the use of Feynman diagram expansion techniques and Wick's theorem.

To see this problem and to proceed beyond it, we take the limit $U \to \infty$, which prevents multiple occupancy of the f-electron state. The Anderson Hamiltonian in this limit may be rewritten using projection operators :

$$\begin{aligned} H = E_0|0,0\rangle\langle 0,0| + \sum_m E_{1,m}|1,m\rangle\langle 1,m| + \sum_{k,m} \mathcal{E}_{\mathbf{k},m} c^\dagger_{\mathbf{k},m} c_{\mathbf{k},m} \\ + \sum_{\mathbf{k},m} (V_k|1,m\rangle\langle 0,0|c_{\mathbf{k},m} + V^*_{\mathbf{k}} c^\dagger_{\mathbf{k},m}|0,0\rangle\langle 1,m| \end{aligned} \tag{2.2}$$

where the energy of a singly occupied f state has been rewritten as the difference in energy between the f state with one particle and angular momentum m, and the f state with no particle:

$$E_{1,m} - E_0 = E_f.$$

Now the possible occupancies and angular momentum for the f-state are enumerated explicitly, with multiple occupancies omitted, due to our assumption of an infinite on-site correlation.

This infinite-U Anderson Hamiltonian actually has an exact solution, based on the Bethe Ansatz [20] [21]. However it requires the unique origin at the single impurity site, so it will not be applicable to us as we try to describe the lattice case, except as a means of comparison for approximate methods in the impurity case.

2.3.2. Hubbard X-operators

The projection operators in the above Hamiltonian can be made to look slightly more familiar with the Hubbard X-operators. A Hubbard X operator is a projection operator

$$X_{0,m} = |00\rangle\langle 1, m|$$

and $\mathrm{Tr}X = I$ by completeness.

The Anderson Hamiltonian in terms of the Hubbard X-operators becomes:

$$H = \sum_{\mathbf{k},m} \mathcal{E}_{\mathbf{k}m} c^{\dagger}_{\mathbf{k}m} c_{\mathbf{k}m} + \sum_{i,m} E_f X_{m,m} + V \sum_{\mathbf{k},m} (c^{\dagger}_{\mathbf{k},m} X_{0,m} + X_{m,0} c_{\mathbf{k},m}). \tag{2.3}$$

While the Hamiltonian looks more like the familiar operator Hamiltonians we're used to, it still contains projection operators. The X operators do not have convenient commutation relations like the creation and destruction operators of fermions and bosons, and as mentioned above, prevent the use of Wick's theorem and diagrammatic expansion techniques. A form of perturbation theory developed by Keiter and Kimball has been used [22], which scales the hybridization parameter, V by $1/\sqrt{N}$, the root of the degeneracy. The expansion in V is then reclassified by the order of $1/N$. This expansion is also difficult to extend from an impurity case to a Kondo lattice.

2.3.3. Slave Bosons

Like the Hubbard X-operators, slave bosons are a useful way of imposing the $U \to \infty$ limit, but without the inconvenient commutation relations. The operators themselves are ordinary fermion and boson creation and destruction operators, rather than projection operators. As is shown below, the slave boson method allows the f orbital to be singly occupied or unoccupied, but never multiply occupied.

The most common formulation of slave bosons in a Kondo problem is by Coleman [23], based on the work of Barnes [24] and Abrikosov [25] who had previously used fictitious slave particles to replace spin and projection operators.

The X-operators are replaced by two operators: one that creates or destroys an electron in the f state, and one that destroys or creates a fictitious boson that is a bookkeeping device preventing multiple occupation of the site.

$$X_{0,m} = b^\dagger f_m \text{ and } X_{m,0} = f_m^\dagger b. \tag{2.4}$$

Loosely, the boson takes up the space on the f site where an f electron could otherwise potentially reside. When there is no electron on the site the spin of the site is zero: There is a boson there. When there is an f electron on the site, the infinite-U approximation dictates that there should not be a spot for a second f electron. So we require that the number of bosons and local fermions on the site sum to unity with the constraint

$$b^\dagger b + \sum_m f_m^\dagger f_m = 1. \tag{2.5}$$

The slave-boson Anderson impurity Hamiltonian is

$$\begin{aligned} H = &\sum_{k,m} \mathcal{E}_{\mathbf{k},m} c_{\mathbf{k},m}^\dagger c_{\mathbf{k},m} + \sum_{\mathbf{k},m} (V_{\mathbf{k}} b f_m^\dagger c_{\mathbf{k},m} + V_{\mathbf{k}}^* b^\dagger f_m c_{\mathbf{k},m}^\dagger) \\ &+ \sum_m E_f f_m^\dagger f_m + \lambda \sum_m (f_m^\dagger f_m + b^\dagger b - 1). \end{aligned} \tag{2.6}$$

Notice the constraint (2.5) is imposed with the Lagrange multiplier λ.

A conventional perturbation expansion in V with the constraint imposed term-by-term is equivalent to the $1/N$ Keiter-Kimball perturbation theory mentioned above. Alternatively, a saddle point approximation can be made by writing the partition function as an integral over the Bose, Fermi, and λ fields [26]. This corresponds to a mean-field approximation such that

$$b^\dagger = \langle b^\dagger \rangle = z = \langle b \rangle = b$$

$$\langle b^\dagger b \rangle = z^2$$

where z is a complex number rather than an operator. The values of λ and z^2 must be determined self consistently (along with the chemical potential, μ, in the lattice model) by minimizing the free energy [27].

This mean-field approximation is exact in the limit of infinite degeneracy. That is, in the limit $N \to \infty$ it corresponds to the $(1/N)^0$ term of the Keiter-Kimball expansion.

For finite N, as the temperature increases the results are affected by the fact that the mean-field approximation only imposes the constraint on the average. Thermal fluctuations which violate the constraint are allowed, so long as it is obeyed in the mean. For cerium the degeneracy of the f state is 14. However spin-orbit splitting reduces this to 6, which is split by the crystal field into a doublet ($N = 2$) and a quartet ($N = 4$).

The mean-field approximation returns the problem to a single-particle problem, since the two-body interaction term which represents the hybridization is simplified when the boson operator becomes a number, and the effect of $U \to \infty$ is replaced by the constraint. The results include the Abrikosov-Suhl resonance mentioned previously. It also allows us to express the Fermi liquid quasi-particle parameters in terms of the bare parameters of the Anderson model.

This model is amenable to extension from an impurity model to a the Kondo lattice, as will be seen in the next section.

2.3.4. The Slave-Boson Anderson Lattice Model

Our approach to the heavy-fermion system, or Kondo lattice, begins with the periodic Anderson model:

$$H = \sum_{k,\sigma} \mathcal{E}_{\mathbf{k},\sigma} c^\dagger_{\mathbf{k},\sigma} c_{\mathbf{k},\sigma} + \sum_{i,\mathbf{k},\sigma,m} \left(V_{\mathbf{k}} e^{i\mathbf{k}\cdot\mathbf{R}_i} f^\dagger_{i,m} c_{\mathbf{k},\sigma} + V^*_{\mathbf{k}} e^{-i\mathbf{k}\cdot\mathbf{R}_i} f_{i,m} c^\dagger_{\mathbf{k},\sigma} \right) \tag{2.7}$$
$$+ \sum_{i,m} \left(E_f f^\dagger_{i,m} f_{i,m} + U f^\dagger_{i,m} f_{i,m} f^\dagger_{i,-m} f_{i,-m} \right).$$

Like the impurity Anderson model, it has particle creation and destruction operators for the conduction electrons and the f-state electrons. The primary difference, of course, is the crystalline sites for the f electrons, labeled by i, corresponding to the Cerium or other rare earth atoms. The hybridization parameter is modified by a phase factor reflecting the fact that the conduction electrons will have a different phase at each site (i.e. Wannier states).

As mentioned above, many of the approximation techniques employed in the impurity problem do not carry over to the lattice case, primarily due to the fact that there is not a unique impurity site to use as an origin. This means we lose total angular momentum conservation about that unique origin. We can no longer honestly describe the conduction electrons and f-electrons as sharing a degeneracy $N = 2J + 1$, since the conduction electrons can't be written in a partial wave expansion about every site. For this reason their angular momentum index can really only be a spin index, $\sigma = \pm\frac{1}{2}$, and all the conduction states are included in the sums.

In the Kondo problem, the conduction states and f states have the same degeneracy, N, which allows the perturabation expansion to be classified by order in $1/N$. This isn't possible in the lattice problem, except in the case where the degeneracy of the f-state is also due only to spin, in which case $N = 2$, which doesn't make $1/N$ a particularly small parameter for expansion. However, this may in fact turn out to be the case once crystal-field splitting is taken into account.

Although our f states may have higher degeneracy than 2, we nonetheless make the assumption of a common degeneracy N to proceed. With this assumption we may write the periodic infinite-U Anderson Hamiltonian as

$$H = \sum_{k,\sigma} \mathcal{E}_{\mathbf{k},\sigma} c^\dagger_{\mathbf{k},\sigma} c_{\mathbf{k},\sigma} + \sum_{i,\mathbf{k},\sigma,m} (V_{\mathbf{k}} e^{i\mathbf{k}\cdot\mathbf{R}_i} b_i f^\dagger_{i,m} c_{\mathbf{k},\sigma} + V^*_{\mathbf{k}} e^{-i\mathbf{k}\cdot\mathbf{R}_i} b^\dagger_i c^\dagger_{\mathbf{k},\sigma} f_{i,m}) + \sum_{i,m} E_f f^\dagger_{i,m} f_{i,m} + \lambda \sum_{i,m} (f^\dagger_{i,m} f_{i,m} + b^\dagger_i b_i - 1). \tag{2.8}$$

We'll treat this in the mean-field approximation, after the work of Newns and Read [28]

$$b^\dagger_i \to \langle b^\dagger_i \rangle = z = \langle b_i \rangle \leftarrow b_i$$

$$\langle b^\dagger_i b_i \rangle = z^2,$$

and in the presence of a magnetic field, which causes a Zeeman splitting, mH, of the f-levels. Finally we convert all the operators to k-space with the Fourier transform

$$f^\dagger_{\mathbf{k},m} = N_s \sum_i e^{i\mathbf{k}\cdot\mathbf{R}_i} f^\dagger_{i,m}, \tag{2.9}$$

where N_s is the number of lattice sites. After dropping the constant terms the Hamiltonian becomes:

$$H = \sum_{\mathbf{k},m} \mathcal{E}_{\mathbf{k},m} c^\dagger_{\mathbf{k},m} c_{\mathbf{k},m} + Vz(f^\dagger_{\mathbf{k},m} c_{\mathbf{k},m} + c^\dagger_{\mathbf{k},m} f_{\mathbf{k},m}) + (E_f + \lambda - mh)(f^\dagger_{\mathbf{k},m} f_{\mathbf{k},m}). \tag{2.10}$$

2.3.5. Green's Matrix

In preparation for the extended Lifshitz-Kosevitch formalism for treating de Haas-van Alphen, we use this Hamiltonian to determine a Green's matrix. Looking at the Hamiltonian we see operators that create two different kinds of particles, so we'll have Green's functions which reflect both these kinds of operators.

This Green's matrix is written:

$$G = \begin{pmatrix} G_{ff}(\zeta_n) & G_{fc}(\zeta_n) \\ G_{cf}(\zeta_n) & G_{cc}(\zeta_n) \end{pmatrix} \tag{2.11}$$

where the matrix elements are functions of imaginary energy $\zeta_n = i\omega_n + \mu$, and for fermions $\omega_n = (2n+1)\pi k_B T$. They are the Fourier sum transforms of the matrix elements in imaginary time, τ:

$$\begin{aligned} G_{ff}(k,\tau) &= -\langle\phi|T_\tau\{f_{k,m}(\tau)f^\dagger_{k,m}(0)\}|\phi\rangle \\ G_{fc}(k,\tau) &= -\langle\phi|T_\tau\{f_{k,m}(\tau)c^\dagger_{k,m}(0)\}|\phi\rangle \\ G_{cf}(k,\tau) &= -\langle\phi|T_\tau\{c_{k,m}(\tau)f^\dagger_{k,m}(0)\}|\phi\rangle \\ G_{cc}(k,\tau) &= -\langle\phi|T_\tau\{c_{k,m}(\tau)c^\dagger_{k,m}(0)\}|\phi\rangle. \end{aligned} \tag{2.12}$$

Imaginary time Green's functions are a feature of Matsubara's method for treating finite-temperature quantum systems. Textbooks which discuss this method include those by Abrikosov, Gorkov, and Dzyaloshinski [29], Mahan [30], and Fetter and Walecka [31]. The angle brackets $\langle ... \rangle$ around the operators indicate a statistical average which is accomplished with a sum over states weighted by a thermodynamic probability operator:

$$\mathrm{Tr}\left(e^{\beta(\Omega_{op}+\mu N_{op}-H_{op})}...\right)$$

$$\beta \equiv \frac{1}{k_B T}.$$

The particle creation and destruction operators are in the Heisenberg representation, e.g.

$$f_{k,m}(\tau) = e^{(H_{op}-\mu N_{op})\tau} f_{k,m}(0) e^{-(H_{op}-\mu N_{op})\tau}. \tag{2.13}$$

The matrix elements are found by using the anti-commutation relations for these fermion operators and their imaginary-time equations of motion.

$$\{f_{k,m}(\tau), c^{\dagger}_{k',m'}(\tau)\} = \delta_{f,c} = 0$$

$$\{f_{k,m}(\tau), f^{\dagger}_{k',m'}(\tau)\} = \delta_{k,k'}\delta_{m,m'} \tag{2.14}$$

$$\frac{d}{d\tau} f_{k,m}(\tau) = [(H_{op} - \mu N_{op}), f_{k,m}(\tau)] \tag{2.15}$$

$$N_{op} = \sum_{k,m} f^{\dagger}_{k,m} f_{k,m} + \sum_{k',m'} c^{\dagger}_{k',m'} c_{k',m'}$$

We start by taking the derivative of the elements of the Green's matrix. The imaginary-time ordering operator, T_τ, in the definition of the Green's functions makes them discontinuous in τ, so their derivatives contain delta functions:

$$\frac{d}{d\tau} G_{ff}(j,\tau) = -\langle\phi|T_\tau\{\frac{df_{j,\sigma}}{d\tau} f^{\dagger}_{j,\sigma}(0)\}|\phi\rangle - \delta(\tau - 0)\delta_{j,j}\delta_{\sigma,\sigma}. \tag{2.16}$$

The time derivative of each of the particle creation and destruction operators is found by evaluating the equal-time commutator in its equation of motion, 2.15, making use of the anti-commutators 2.14 and the Hamiltonian 2.10. For example, $[H, f_{j,\sigma}]$ contains the term $(E_f + \lambda - mh)[f^{\dagger}_{k,m} f_{k,m}, f_{j,\sigma}]$, which must be evaluated:

$$\begin{aligned}
[f^{\dagger}_{k,m} f_{k,m}, f_{j,\sigma}] &= f^{\dagger}_{k,m} f_{k,m} f_{j,\sigma} - f_{j,\sigma} f^{\dagger}_{k,m} f_{k,m} \\
&= f^{\dagger}_{k,m} f_{k,m} f_{j,\sigma} - (\delta_{j,k}\delta_{m,\sigma} - f^{\dagger}_{k,m} f_{j,\sigma}) f_{k,m} \\
&= f^{\dagger}_{k,m} f_{k,m} f_{j,\sigma} - \delta_{j,k}\delta_{m,\sigma} f_{k,m} + f^{\dagger}_{k,m}(-f_{k,m} f_{j,\sigma}) \\
&= \delta_{j,k}\delta_{m,\sigma} f_{k,m}.
\end{aligned} \tag{2.17}$$

In this way a set of coupled equations for the Green's functions in imaginary time is found:

$$\begin{aligned}
\frac{d}{d\tau} G_{ff}(j,\tau) &= (E_f + \lambda - mh - \mu)(-G_{ff}(j,\tau)) - Vz G^{\dagger}_{fc}(j,\tau) - \delta(\tau - 0) \\
\frac{d}{d\tau} G_{fc}(j,\tau) &= (E_f + \lambda - mh - \mu)(-G_{fc}(j,\tau)) - Vz G_{cc}(j,\tau) \\
\frac{d}{d\tau} G_{cc}(j,\tau) &= (\mu - \mathcal{E}_{km})(G_{cc}(j,\tau)) - Vz G_{fc}(j,\tau) - \delta(\tau - 0),
\end{aligned} \tag{2.18}$$

where $G^{\dagger}_{fc} = G_{cf}$. These may be easily solved once Fourier transformed from imaginary time to imaginary energy,

$$G(\tau) = k_B T \sum_n e^{-i\omega_n \tau} G(\omega_n), \tag{2.19}$$

$$G(\omega_n) = \frac{1}{2}\int_{-\beta}^{\beta} e^{i\omega_n \tau} G(\tau) d\tau,$$

$$\omega_n = (2n+1)\pi k_B T,$$

$$\beta \equiv \frac{1}{k_B T},$$

which yields the matrix elements

$$G_{ff}(\zeta_n) = \left(\zeta_n - (E_f + \lambda - mh) - \frac{V^2 z^2}{\zeta_n - \mathcal{E}_{km}}\right)^{-1}$$

$$= \frac{\zeta_n - \mathcal{E}_{km}}{(\zeta_n - \mathcal{E}_{km})(\zeta_n - (E_f + \lambda - mh)) - V^2 z^2} \tag{2.20}$$

$$G_{fc}(\zeta_n) = G_{cf} = \frac{Vz}{(\zeta_n - \mathcal{E}_{km})(\zeta_n - (E_f + \lambda - mh)) - V^2 z^2} \tag{2.21}$$

$$G_{cc}(\zeta_n) = \left(\zeta_n - \mathcal{E}_{km} - \frac{V^2 z^2}{\zeta_n - (E_f + \lambda - mh)}\right)^{-1}$$

$$= \frac{\zeta_n - (E_f + \lambda - mh)}{(\zeta_n - \mathcal{E}_{km})(\zeta_n - (E_f + \lambda - mh)) - V^2 z^2}. \tag{2.22}$$

If these Green's functions are analytically continued back to the real-energy axis it is seen that they have poles at energy, E, where

$$(E - \mathcal{E}_{km})(E - (E_f + \lambda - mh)) - V^2 z^2 = 0. \tag{2.23}$$

The solutions to this quadratic equation (with $h = 0$) are the renormalized bands pictured in figure 2.1. The Lagrange multiplier from the constraint renormalizes the f state upward by an amount λ so that it crosses the conduction band. The hybridization between these states breaks the conduction band into the two bands, with the Fermi energy lying just below the renormalized f state, in the flat portion of the lower band.

3. SUPERCONDUCTIVITY AND THE VORTEX STATE

3.1. Properties of Superconductors

A superconductor is a new phase of matter that exists in some materials at low temperatures (i.e. below some critical temperature). In the superconducting state, paired electrons exhibit coherent properties akin to those of coherent photons in a laser: the electrons have good phase, but their number (how many of them are in this state) is not conserved. The paired electrons in this coherent state are collectively called the condensate, and are all described by a single wave function, called the order parameter or the pairing wave function. The origin of the unique behavior of superconductors lies in the pairing of electrons. Electrons are fermions, obeying the Pauli exclusion principle. However when paired, their combined angular momenta may be integral so they behave like bosons, able to condense into a single quantum state. The source of the pairing in many superconducting materials is an attractive interaction between electrons mediated by phonons. Other interactions have been postulated, particularly for the heavy fermion and high temperature superconductors, but none have been proven conclusively.

The condensate does not contain all the electrons in a solid. It is made up of those electrons which lie near the Fermi surface. Those electrons which remain (the "normal" electrons) interact with the condensate, which modifies their density of states. The normal electrons have no states available to them near the Fermi surface, approximately within the range of twice the pairing energy. That is to say, there is a gap in the density of states. The size of the gap in the absence of a magnetic field is proportional to the magnitude of the order parameter describing the superconducting electrons.

The two most dramatic manifestations of superconductivity are infinite conductivity and the expulsion of magnetic fields. The infinite conductivity is due to the gap in the density of states. If the temperature is low enough ($kT < \Delta$) thermal scattering will not be energetic enough to scatter electrons from the coherent condensate into normal states.

The magnetic flux expulsion is a result of the coherence of the condensate, and the magnetic vector potential. Flux in the body of the superconductor increases the energy of the state. To avoid this increase in energy, surface supercurrents are generated which create an opposing magnetization. The magnetic field, B, falls off exponentially with distance from the surface of the material, characterized by a penetration depth, λ.

3.2. Type-II Superconductors and the Vortex State

Both the magnetic field and the order parameter are solutions of differential equations, and they vary smoothly. The penetration depth (λ) of a superconductor reveals the distance over which the magnetic field,B, changes. It reveals how much energy is required to support a magnetic field inside the superconductor. The coherence length (ξ) is another parameter characterizing a superconducting material. It describes the length over which the order parameter changes, or how much energy is required to perturb the order parameter.

The ratio of these two characteristic lengths, $\kappa = \lambda/\xi$, is called the Ginzburg-Landau ratio. If the flux expulsion is very strong or if the order parameter can change only over large distances, the penetration depth is small compared to the coherence length and the Ginzburg-Landau ratio is small. In this case ($\kappa < 1/\sqrt{2}$) the magnetic field is expelled completely unless it is such a strong field that it

destroys the superconducting state. This is a type-I superconductor, which has one critical field, i.e. for $H > H_c$ the superconductivity disappears.

If the order parameter can change easily over short distances compared to the magnetic field, the Ginzburg-Landau ratio is large ($\kappa > 1/\sqrt{2}$) . In this case the flux will be completely expelled for fields smaller than a lower critical field, H_{c1}. But at fields somewhat larger than H_{c1}, the superconductor will allow the flux to penetrate it, forming cylinders of normal material. Supercurrents around each cylinder localize the flux within the penetration depth, and inspire the name"vortices". As we'll see, these vortices avoid each other and arrange themselves in a lattice. Alexei Abrikosov shared the 2003 Nobel Prize in Physics for predicting this vortex lattice, before any materials with a large Ginzburg-Landau ratio were even known [32].

If larger fields are applied to these type-II superconductors the normal regions grow until superconductivity is again destroyed at an upper critical field, H_{c2}. However in the intermediate "vortex state" or "mixed state", the superconductivity is present but altered. The superconducting energy gap in the density of states for the normal electrons disappears for electrons travelling perpendicular to the magnetic field [33]. These electrons have states at the Fermi surface, which will be crucial for the de Haas-van Alphen experiment. The gap remains for electrons travelling parallel to the field, and decreases smoothly as a function of direction to the gapless state for perpendicular travel. The order parameter is altered in the vortex state, and will reflect the periodicity of the lattice of vortices.

In the materials we are concerned with, the penetration depth is large enough that the normal electrons are not localized within the vortex cores. The de Haas-van Alphen "orbits" encompass many vortices.

3.3. Unconventional Superconductors

Bardeen, Cooper and Schrieffer gave the first theory of superconductivity, based on electron pairing mediated by phonons [34]. This theory describes most superconducting materials discovered to date, the "conventional" superconductors. Extensions of BCS theory exist which describe more unconventional nodal superconductors as well [35].

In conventional superconductors the order parameter is spherically symmetric in momentum space (and real space). Since s orbitals (the $l = 0$ state of a particle in a spherically symmetric potential) are also spherically symmetric these conventional superconductors are called "s-wave" superconductors. However the order parameter may have other behaviors in momentum space, which correspond to the $l = 1, 2, 3...$ states and their associated spherical harmonics. These are called "p-wave", "d-wave", "f-wave", et cetera, and these materials are termed unconventional superconductors. [1]

These symmetries are based on free electrons, so are only approximate in real superconducting materials in which neither orbital nor spin angular momentum

---

[1]The precise definition of what makes an order parameter unconventional is not completely uniform. Some use this definition of the angular momentum of the Cooper pair, but other definitions include; the presence of nodes in the order parameter, broken symmetries in addition to gauge symmetry, or an order parameter which averages to zero over the fermi surface. Usually, but not always, these features appear together in an "unconventional" superconductor. The term may also refer to any departure from the BCS theory (e.g. non-isotropic or novel pairing mechanisms), but extensions of the original theory to describe these now common materials makes this definition less precise [36], [37], [38], [35].

are good quantum numbers due to the crystal lattice. Nonetheless they provide the basic concepts for understanding superconducting materials. (A nice review of the characteristics of unconventional pairing as applied to the problem of Sr_2RuO_4 is given by Mackenzie and Maeno [38]. Specific densities of states and the power laws for various gaps with line and point nodes, as well as gap equations relevant to electrons in a real crystal are given by Joynt and Taillefer. [39])

Since the elementary excitations in a superconductor (the electrons) are fermions, the wave function (or Green's function) which describes them must be antisymmetric under exchange of particles. The even angular momentum states are symmetric under exchange, while the odd states are antisymmetric. Therefore the spin state of the pairing electrons must be antisymmetric for the even-angular-momentum states, and vice versa. Correspondingly, s-, d-, or g-wave superconductors have paired electrons in the antisymmetric spin singlet states (S=0), while a p- or f-wave superconductor requires triplet pairing (S=1).

The primary characteristic of the superconducting state is good phase, i.e. coherent states. Therefore the superconducting state breaks gauge symmetry in all cases. In the higher angular-momentum pairing states (beyond $l = 0$) additional symmetries may be broken, including rotation symmetries applicable to the crystal lattice (and free space) or time-reversal symmetry (due to the net angular momentum of a triplet state).

There is only one function corresponding to the spherically symmetric s-wave order parameter. However the higher angular momentum classifications have many possible functions which fall within "p-wave", "d-wave", et cetera. The functions are often specified by their group-theory symmetry class.

3.3.1. Determining the Symmetry of the Order Parameter

Unpaired electrons obviously have a net spin (S=$\frac{1}{2}$). So a superconducting transition to a singlet paired state (S = 0) will isotropically reduce the magnetic susceptibility of the itinerant electron system (the Pauli spin susceptibility). The NMR Knight shift is the shift in the resonant frequency of a nuclear spin specifically due to the magnetization of the itinerant electrons. The magnetization changes the magnetic field felt by the nucleus. The Knight shift is proportional to the Pauli spin susceptibility, and so can determine whether a superconducting transition is to a singlet or triplet state. Likewise, scattering with polarized neutrons or muon spin resonance experiemnts can measure this susceptibility and indicate the same thing.

In s-wave superconductors the phase of the order paramater is constant for all directions in momentum-space. The magnitude is, in principle, spherically symmetric although effects of the lattice may alter this somewhat. In the unconventional pairing states the gap function (usually) has nodes, where the magnitude goes to zero, and the phase varies for different directions in k-space. In fact, the phase varies such that the average value of the gap function over all directions is zero.

$$\sum_{k} \Delta(\vec{k}) = 0$$

One implication of this is that elastic scattering destroys the order parameter, and only very pure materials display superconductivity, with impurities supressing the transition temperature. Elastic scattering does not impact a conventional order parameter in this way, since the entire gap has the same phase, so mixing does not affect coherence.

Any isotropic order parameter (s-wave or certain d-wave states in 2-dimensions) has the gap Δ in the density of states for every $\vec{k}$ direction. This means that at temperatures below $0.4T_c$ (where the BCS order parameter is very

nearly fully developed and changes little with temperature) the number of thermally excited quasiparticles in energy states above the gap ("normal electrons") vanishes exponentially, and so do the electronic specific heat (c_p), NMR nuclear spin relaxation rate ($\frac{1}{T_1}$), thermal conductivity (κ) and penetration depth (λ). The presence of nodes in the order parameter means that there are states near the Fermi energy in certain directions, and these same quantities display power law decreases, rather than exponential ones. Experiments which average the size of the gap still show BCS behavior [40].

Tunnelling experiments measure the density of states directly, and so can directly measure the gap. However they are highly dependent on the quality of the junction, thus the interpretation of any individual experiment can be subject to dispute [41] [42].

A recent method for examining the shape of the order parameter uses angular resolved magnetothermal transport measurements. A magnetic field is applied in various directions within a plane of the crystal. The thermal conductivity perpendicular to the plane is measured as a function of the orientation of the field within the plane. The basis of the experiment is the change in the density of states due to the vortex state. One way of understanding it is in terms of the Volovik effect [43], in which the energy of quasiparticles (normal electrons) is Doppler shifted as a result of their motion with respect to the supercurrent induced by the magnetic field. $E(\vec{p}) \rightarrow E(\vec{p}) - \vec{v}_{sc} \cdot \vec{p}$. When the Doppler shift is larger than the gap for a certain direction, there is an additional contribution to the density of states at the Fermi energy from momentum states that would otherwise be in the gap. The additional DOS contribution is largest when $\vec{v}_{sc} \cdot \vec{p}$ evaluated at the nodes (where the gap goes to zero) has its largest value. The supercurrent is perpendicular to the magnetic field, so when the field direction is parallel to the momentum at a node,

$\vec{v}_{sc} \perp \vec{p}$ and this node does not contribute anything additional to the DOS. The result is an oscillation in the thermal conductivity as the direction of the field is rotated and the angle with respect to the nodal momenta changes [41]. Predictions can thus be made for the angular dependence of the magnetothermal conductivity for several candidate order parameters and compared to experiment.

The explanation above is described in terms of quasiparticles interacting with a single vortex and its supercurrent. It is only appropriate at low fields (near H_{c1}). As the field increases so does the density of vortices, and scattering off the vortex lattice must be taken into account as well as the Doppler shift [44]. In this case the Brandt, Pesch and Tewordt Green's function for electrons interacting with a vortex lattice that we use in section 3.4 is more appropriate. It takes into account the Doppler shift and vortex-lattice scattering, although the latter only in a spatially averaged way. It shows clearly an additional effect: the density of states, even for a spherically symmetric order parameter, has the full superconducting gap only for quasiparticle motion parallel to the field. Particles moving perpendicular to the field have a more uniform, nearly gapless, density of states. [33] This suppression of the gap makes the Doppler shift much less noticable, so theoretical calculations which take it into account often predict indistinguishable results for several candidate order parameters [45]. In general, the interpretation of these experiments is subject to debate based on the different theoretical models used to predict the results [41], [45], [44], [46].

3.3.2. The Order Parameter of Heavy-Fermion Superconductors

Heavy-fermion superconductivity is not of the conventional s-wave variety. However there is no consensus for the precise symmetry of the order parameter of

any of the heavy-fermion materials. The strong on-site repulsion responsible for the heaviness is also expected to prevent s-wave pairing. An anisotropic pairing state allows the heavy electrons less overlap.

The first experimental evidence of exotic superconductivity in a heavy fermion material was seen by Ott, et al. [47] as a T^3 dependence of the specific heat of UBe_{13}. Since that time many of the heavy fermion materials have shown at least some of the characteristics of non s-wave superconductivity mentioned in the previous paragraph. Since triplet superconductivity is relatively rare, signs of its appearance in UPt_3 have been followed with interest. Triplet superconductivity is necessarily unconventional. Strong evidence of an unconventional pairing state is observed in UPt_3, including the observation of multiple superconducting phase transitions [48] (There is only one possible pairing state for an s-wave superconductor, while there are many possible p-wave and d-wave states due to internal degrees of freedom in the paired state.) The specific heat shows a T^2 dependence characteristic of a gap with line nodes [49]. Asymmetry of ultrasound attenuation [50] implies an asymmetric gap, as do the NMR relaxation rate [51], and penetration depth [52]. Furthermore, measurements of the NMR Knight shift as a function of crystal orientation show an anisotropic reduction of the Pauli spin susceptibility in the superconducting state. This has been interpreted as indicative of a triplet p-wave order parameter which locks to the lattice, causing the direction of the net angular momentum of the pairs ($S = 1$) to depend on the orientation of the crystal axes with respect to the applied magnetic field [53], [54], [55], [42]. Figure 3.1 from Brison, et al. [42] shows a phase diagram of UPt_3 with possible order parameters illustrated for the three different superconducting phases.

There are four heavy fermion superconductors in which the de Haas-van Alphen effect has been observed in the superconducting state: UPd_2Al_3 [56] [57],

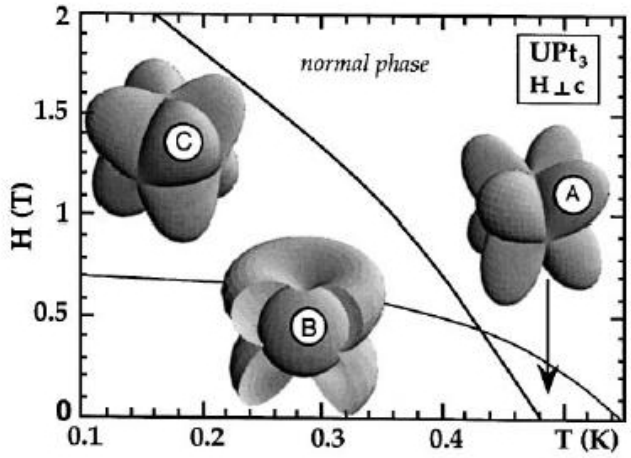

FIGURE 3.1. Phase diagram and order parameters for UPt_3 [42].

$CeRu_2$ [58] [59], URu_2Si_2 [60] [61] [14] [62] [57], and $CeCoIn_5$ [63]. The last is a layered material in which the two-dimensional confinement of electrons is expected to play a significant role. Because of this complication, we are primarily concerned with the other three.

The order parameter for UPd_2Al_3 is not known definitively, however it is almost certainly an even parity function (singlet pairing). This is evidenced by phase coherence in a junction with superconducting niobium (an s-wave superconductor) [64]; and a reduction in the spin susceptibility in the superconducting state as measured by μSR [65] and an isotropic reduction of the Knight shift in NQR [66]. The specific heat has a T^3 dependence [11] [67], which would be consistent with point nodes in the order parameter. However all other experiments indicate line nodes. The discrepancy is possibly due to the fact that magnetic degrees of freedom, in addition to the electronic ones, contribute to the specific heat. Experimental evidence for line nodes in the order parameter include: the nuclear spin lattice relaxation rate ($\frac{1}{T_1} \sim T^3$) [66]; thermal conductivity and resistivity ($\sim T^2$)

[68]; and angularly resolved magnetothermal transport measurements [41]. Normal-Insulating-Superconducting junction spectroscopy with thin films has been used to measure the c-axis density of states which shows a gap (not a node) [69]. Brison [42] claims that all even parity states with lines of nodes have nodes on the c-axis, and concludes that there should be a line of nodes at $k_z = \pm\frac{Q}{2}$ due to antiferromagnetic order rather than a breaking of the symmetry of the lattice by the superconducting state. Q corresponds to the momentum transfer to an antiferromagnetic spin wave at 1.5 meV observed in inelastic neutron scattering [70]. However no subsequent authors seem to have trouble finding even parity states with horizontal line nodes.

The magnetothermal transport experiments show no nodal oscillation of κ_{zz} when the field is rotated in the basal (a-b) plane, so a cylindrically symmetric order parameter is concluded. A two-fold oscillation in κ_{yy} as the field is rotated in the plane perpendicular to the basal plane indicated horizontal line nodes. However there is no agreement on which candidate order parameter is the best match for experiment. Watanabe [41] and Thalmeier [71] pay particular attention to the shape of the Fermi surface at the gap nodes and conclude that it is the d-wave A_{1g} order parameter $\Delta = \Delta_o \cos(ck_z)$ (c is the z-axis lattice parameter). Won [46] and Maki [72] conclude that it is the g-wave $A_{1g} \oplus A'_{1g}$, $\Delta = \Delta_o \cos(2ck_z)$. Tewordt and Fay [45] include Andreev scattering off the vortex cores in their calculation and find that four candidate gap functions (the two above, $\Delta = \Delta_o \sin(2ck_z)$, and $\Delta = \Delta_o \sin(ck_z)$) are consistent with the experiment.

The magnetic phase of URu_2Si_2 is far more studied than the superconducting phase. Antiferromagnetism with a tiny moment ($0.3\mu_B$) is seen, along with a specific heat jump at the Neel temperature consistent with far more order than implied by the tiny moment [73]. The"hidden order" is speculated to be an unconventional spin density wave, whose gap is momentum dependent (as the superconducting

gap is in an unconventional superconductor) [74]. The superconductivity in this material is also likely unconventional. The specific heat has a T^2 dependence [75], and the NMR/NQR relaxation rate $\frac{1}{T_1}$ has a T^3 dependence, with no coherence peak [76], both of which are consistent with line nodes in the superconducting gap. The competition between an unconventional density wave order parameter and an unconventional superconducting order parameter has been suggested to lead to "gossamer superconductivity", with a very small superfluid density and a very small spectral weight [77], [78] in URu_2Si_2 and UPd_2Al_3.

The temperature dependence of the specific heat of $CeRu_2$ suggests an order parameter with nodes [79], while NQR suggests s-wave pairing [80]. Experiments which try to measure the gap directly (point contact spectroscopy [81], scanning tunnelling spectroscopy and microscopy [82], and break junction tunnelling [83] are consistent with BCS behavior (no nodes).

The unconventional order parameter of the heavy-fermion superconductors begets the question of unconventional pairing. As mentioned above, pairing of electrons in BCS superconductors is mediated by phonons. The strong correlations and the resulting magnetic moments which are fundamental to the heavy fermion behavior imply the possibility of some sort of magnetically mediated pairing interaction. One possible mediator is a spin fluctuation, an excitation in which an electron temporarily reverses its spin due to an interaction with a virtual electron. These fluctuations can lead to an antiferromagnetic transition in the itinerant electrons by the creation of a spin density wave (UPt_3). Another is magnetic excitons or magnons, (UPd_2Al_3), which are excitations of the localized spins (electrons) near an antiferromagnetic transition whose interactions are mediated by itinerant electrons [84] [85] [86] [87] [88].

The coexistence of antiferromagnetism and superconductivity in these materials as well as many other unconventional superconductors (including the high T_c superconductors) has led to the postulate that the antiferromagnetism and superconductivity might share a common origin. Their separate order parameters might be different manifestations of a single unified order parameter, the superspin. [89]

3.4. Calculation of the Green's Function in the Vortex State

The de Haas-van Alphen effect is an oscillation of the magnetization as the applied magnetic field changes. It depends upon having electrons at the Fermi surface. Thus it is type-II superconductors in the vortex state which may be studied with de Haas-van Alphen.

We'll calculate the Green's function of such a superconductor in the vortex state following the work of Abrikosov [32], (Helfand and Werthamer [90]), Linden-Levy [91], Brandt [33], and Wasserman [92].

We assume that we are near the upper critical field, $H \sim H_{c2}$, and that the magnetic field inside the superconductor is slowly varying in space compared to the Green's function and the coherence length. We evaluate the Green's functions only to first order in magnetic field.

The superconductor is described by the Ginzburg-Landau (G-L) equations, which assume only that there is a short-range attractive interaction between electrons near the Fermi surface, which leads to pairing.

We'll use the G-L equations to obtain differential and integral equations for the order parameter and the Green's function in terms of the order parameter, valid to first order in the order parameter. The differential equation for the order parameter is solved. The integral equation for the Green's function is transformed

to momentum space, and we make approximations relevant to the conditions of the de Haas-van Alphen experiment in order to evaluate it.

First some definitions: $G(\mathbf{r}, \mathbf{r}'; \omega_n)$ is the full Green's function for a superconductor in a magnetic field; $G^0(\mathbf{r}, \mathbf{r}'; \omega_n)$ is the Green's function for normal electrons in a magnetic field; $G^{00}_{(\mathbf{r}-\mathbf{r}')}$ is the Green's function for normal electrons in the absence of a magnetic field. (Note the Green's function for free particles in the absence of external fields is only a function of $\mathbf{r} - \mathbf{r}'$.) As usual, $\omega_n = (2n+1)\frac{\pi}{\beta}$, $\beta = \frac{1}{k_B T}$ and $\mathbf{r}$ and $\mathbf{r}'$ are position variables. Each of these Green's functions is the Fourier transform of an imaginary-time Green's function

$$G(\mathbf{r}, \mathbf{r}'; \tau - \tau') = -\langle T_\tau \{\psi(\mathbf{r}, \tau)\psi^\dagger(\mathbf{r}', \tau')\}\rangle \tag{3.1}$$

where the ψ are field functions for conduction electrons. We occasionally drop the ω_n when it is not immediately relevant.

3.4.1. The Effect of a Magnetic Field

We begin with the equations of motion for normal electrons both in the absence and presence of a magnetic field .

$$\left[i\omega_n + \mu + \frac{1}{2m}\nabla^2_{\mathbf{r}} \right] G^{00}_{(\mathbf{r}-\mathbf{r}')} = \delta(\mathbf{r} - \mathbf{r}') \tag{3.2}$$

$$\left\{ i\omega_n + \mu + \frac{1}{2m}\left[\nabla_{\mathbf{r}} - \frac{ie}{\hbar}\mathbf{A}(\mathbf{r}) \right]^2 \right\} G^0(\mathbf{r}, \mathbf{r}') = \delta(\mathbf{r} - \mathbf{r}') \tag{3.3}$$

We then postulate that to first order in the magnetic field, the field only changes the Green's function by a phase:

$$G^0_{(\mathbf{r},\mathbf{r}')} = e^{\varphi(\mathbf{r},\mathbf{r}')} G^{00}_{(\mathbf{r}-\mathbf{r}')}.$$

By making this substitution, equation 3.3 becomes:

$$-2m\left[e^{\varphi(\mathbf{r},\mathbf{r}')}(i\omega_n+\mu)G^{00}_{(\mathbf{r}-\mathbf{r}')}-\delta(\mathbf{r}-\mathbf{r}')\right]=\left[\nabla_r-\frac{ie}{\hbar}\mathbf{A}(\mathbf{r})\right]^2 e^{\varphi(\mathbf{r},\mathbf{r}')}G^{00}_{(\mathbf{R})},$$

where $\mathbf{R}\equiv\mathbf{r}-\mathbf{r}'$.

Examining the right hand side of this equation to first order in A in the gauge $\nabla\cdot\mathbf{A}=0$ yields:

$$\begin{aligned}RHS=&\left(\nabla^2\varphi\right)e^{\varphi}G^{00}(\mathbf{R})+\left(\nabla\varphi\right)^2e^{\varphi}G^{00}(\mathbf{R})+2e^{\varphi}\nabla\varphi\cdot\nabla G^{00}(\mathbf{R})\\&+e^{\varphi}\nabla^2G^{00}(\mathbf{R})-\frac{2ie}{\hbar}\mathbf{A}(\mathbf{r})\cdot\left[\left(\nabla\varphi\right)e^{\varphi}G^{00}(\mathbf{R})+e^{\varphi}\nabla G^{00}(\mathbf{R})\right].\end{aligned}$$

Applying Gauss's theorem (the divergence theorem) we obtain:

$$e^{\varphi}(i\omega_n+\mu)G^{00}_{(\mathbf{r}-\mathbf{r}')}-\delta(r-r')=\frac{1}{2m}e^{\varphi}\left[\nabla^2G^{00}_{(\mathbf{r}-\mathbf{r}')}+\left(2\nabla\varphi-\frac{2ie}{\hbar}\mathbf{A}\right)\cdot\nabla G^{00}_{(\mathbf{r}-\mathbf{r}')}\right]. \tag{3.4}$$

Applying equation 3.2 to eliminate several terms in this equation yields:

$$\hat{n}\cdot\nabla\varphi=\hat{n}\cdot\mathbf{A}\left(\frac{ie}{\hbar}\right) \tag{3.5}$$

where

$$\hat{n}\equiv\frac{\nabla G^{00}_{(\mathbf{r}-\mathbf{r}')}}{\left|\nabla G^{00}_{(\mathbf{r}-\mathbf{r}')}\right|}. \tag{3.6}$$

With $G^{00}_{(\mathbf{r}-\mathbf{r}')}$ the free state Green's function,

$$\hat{n}=\hat{R}.$$

This equation for the phase may also be written

$$\varphi(\mathbf{r},\mathbf{r}')=\frac{ie}{\hbar}\int_{\mathbf{r}'}^{\mathbf{r}}\mathbf{A}(\mathbf{r})\cdot\mathbf{dr}. \tag{3.7}$$

For our purposes we'll be dealing with a magnetic field of strength H in the $\hat{z}$-direction, and the Coulomb gauge. Specifically, we'll choose:

$$\mathbf{A} = xH\hat{y} \tag{3.8}$$

Since the magnetic field varies slowly in space we can approximate it as the average of its values at the two endpoints of the integral, which yields for the phase:

$$\varphi(\mathbf{r}, \mathbf{r}') = \frac{ieH}{\hbar}\frac{(r_x + r'_x)}{2}(r'_y - r_y) \tag{3.9}$$

3.4.2. The Gorkov Equations for a Superconductor

Superconducting electrons in a magnetic field satisfy the mean-field Gorkov equations:

$$\left(i\omega_n + \frac{1}{2m}[\nabla_{\mathbf{r}} - ie\mathbf{A}(\mathbf{r})]^2 + \mu\right) G_\omega(\mathbf{r}, \mathbf{r}') + \Delta(\mathbf{r})F^\dagger_\omega(\mathbf{r}, \mathbf{r}') = \delta(\mathbf{r} - \mathbf{r}') \tag{3.10}$$

$$\left(-i\omega_n + \frac{1}{2m}[\nabla_{\mathbf{r}} + ie\mathbf{A}(\mathbf{r})]^2 + \mu\right) F^\dagger_\omega(\mathbf{r}, \mathbf{r}') - \Delta^*(\mathbf{r})G_\omega(\mathbf{r}, \mathbf{r}') = 0 \tag{3.11}$$

$$\Delta^*(\mathbf{r}) \equiv |\lambda| T \sum_\omega F^\dagger_\omega(\mathbf{r}, \mathbf{r}) \tag{3.12}$$

$F^\dagger$ is a new kind of Green's function, that corresponds to (conduction) electron pairs ($\psi^\dagger\psi^\dagger$), rather than the propogation of a single electron like a regular Green's function ($\psi\psi^\dagger$).

$$F^\dagger(\mathbf{r}, \mathbf{r}'; \tau - \tau') = -\langle T_\tau\{\psi^\dagger(\mathbf{r}, \tau)\psi^\dagger(\mathbf{r}', \tau')\}\rangle \tag{3.13}$$

$$F(\mathbf{r}, \mathbf{r}'; \tau - \tau') = -\langle T_\tau\{\psi(\mathbf{r}, \tau)\psi(\mathbf{r}', \tau')\}\rangle$$

Δ is the order parameter for the superconductor, which is something like the number of pairs of electrons. (As we discussed previously, particle number is not a good

quantum number in the superconducting state.) λ represents a coupling strength for the electron-electron interaction responsible for pairing.

As can be verified by direct substitution into Gorkov's equations, we can write the Green's functions as integral equations in terms of $G^{0}_{(\mathbf{r},\mathbf{r}')}$:

$$G_{(\mathbf{r},\mathbf{r}')} = G^{0}_{(\mathbf{r},\mathbf{r}')} - \int G^{0}_{(\mathbf{r},\mathbf{l})}\, \Delta(l)\, F^{\dagger}(\mathbf{l},\mathbf{r}')\, d\mathbf{l} \tag{3.14}$$

$$F^{\dagger}(\mathbf{r},\mathbf{r}') = \int G^{0}_{-\omega(\mathbf{l},\mathbf{r})}\, \Delta^{*}(\mathbf{l})\, G_{(\mathbf{l},\mathbf{r}')}\, dl. \tag{3.15}$$

Which can be combined to become:

$$G_{(\mathbf{r},\mathbf{r}')} = G^{0}_{(\mathbf{r},\mathbf{r}')} - \int d\mathbf{l} \int d\mathbf{l}'\, G^{0}_{(\mathbf{r},\mathbf{l})}\, \Delta(\mathbf{l})\, G^{0}_{-\omega(\mathbf{l},\mathbf{l}')}\, \Delta^{*}(\mathbf{l}')\, G_{(\mathbf{l}',\mathbf{r}')}. \tag{3.16}$$

(The terms which do not have subscripts are still functions of ω_n, but this has been suppressed for brevity.)

To evaluate this expression for the Green's function we need the order parameter, which, in turn, depends on the Green's function. So we apporximate the full, superconducting, Green's function with the non-superconducting Green's function for the purposes of finding the order parameter. This will then eventually be substituted back into the expression for the full Green's function, which expression will now be correct only to first order in the order parameter. The approximation of the equation for the order parameter is:

$$\Delta^{*}(\mathbf{r}) \approx |\lambda| \int e^{2\varphi(\mathbf{l},\mathbf{r})}\, K^{00}(\mathbf{l}-\mathbf{r})\, \Delta^{*}(\mathbf{l})\, d\mathbf{l},$$

where

$$K^{00}(\mathbf{l}-\mathbf{r}) \equiv T \sum_{\omega_n} G^{00}_{-\omega(\mathbf{l}-\mathbf{r})} G^{00}_{(\mathbf{l}-\mathbf{r})}.$$

This "kernel" of the free electron Green's function has an exponential form:

$$K^{00}(\mathbf{l}-\mathbf{r}) \sim e^{-|\omega_n||\mathbf{R}|/v}$$

$$\mathbf{R} \equiv \mathbf{l} - \mathbf{r},$$

so the largest contribution to the integral occurs near $\mathbf{l} = \mathbf{r}$ or $\mathbf{R} = 0$. So we'll expand the other two terms in the integral around this point.

For small $\mathbf{R}$, the phase may be approximated by

$$\varphi(\mathbf{l}, \mathbf{r}) \approx \frac{ie}{\hbar}\mathbf{A} \cdot \mathbf{R},$$

and the expansion of the phase exponential is the standard power series.

To expand the order parameter around the point $\mathbf{R} = 0$ it needs to be written in terms of $\mathbf{R}$:

$$\Delta^*(\mathbf{l}) = \Delta^*(\mathbf{R} + \mathbf{r}) \approx \Delta^*(\mathbf{r}) + \mathbf{R} \cdot \nabla_{\mathbf{u}} \Delta^*(\mathbf{u})\big|_{\mathbf{r}} + \frac{1}{2!}\left(\sum_{i,j} R_i R_j \frac{\partial^2 \Delta^*(\mathbf{u})}{\partial u_i \partial u_j}\right)_{\mathbf{r}} + ...$$

Multiplying the two expansions and arranging the result in increasing order of R yields:

$$\begin{aligned}
\Delta^*(\mathbf{r}) \approx\ & |\lambda| \int d\mathbf{l} K^{00}(\mathbf{l} - \mathbf{r}) \Delta^*(\mathbf{r}) && \text{0th order} \\
& + |\lambda| \int d\mathbf{l} K^{00}(\mathbf{R}) \left(\Delta^*(\mathbf{r}) \frac{2ie}{\hbar}(\mathbf{A} \cdot \mathbf{R}) + \mathbf{R} \cdot \nabla_{\mathbf{u}} \Delta^*(\mathbf{u})\big|_{\mathbf{r}}\right) && \text{1st order} \\
& + |\lambda| \int d\mathbf{l} K^{00}(\mathbf{R}) \left[-\Delta^*(\mathbf{r}) \frac{2e^2}{\hbar^2}(\mathbf{A} \cdot \mathbf{R})^2 + \left(\mathbf{R} \cdot \nabla_{\mathbf{u}} \Delta^*(\mathbf{u})\big|_{\mathbf{r}}\right)\left(\frac{2ie}{\hbar}\mathbf{A} \cdot \mathbf{R}\right)\right. \\
& \qquad \left. + \frac{1}{2}\sum_{i,j} R_i R_j \frac{\partial^2 \Delta^*(\mathbf{u})}{\partial u_i \partial u_j}\bigg|_{\mathbf{r}}\right]. && \text{2nd order}
\end{aligned} \tag{3.17}$$

The first order term is zero once integrated, because $\mathbf{A}$ and $\nabla\Delta|_{\mathbf{r}}$ are functions of $\mathbf{r}$ only. They are therefore fixed vector fields with respect to the integration, and the dot product with $\mathbf{R}$ will average to zero over all solid angle.

To examine the three integrals that make up the second order term we first note that $K^{00}(\mathbf{R})$ depends only on $|\mathbf{R}|$ and $d\mathbf{l} = d\mathbf{R}$. This allows us to simplify the first integral:

$$I_1 \equiv \int (\mathbf{A}\cdot\mathbf{R})^2 K^{00}(|\mathbf{R}|)\, d\mathbf{R}$$
$$= \int |A|^2|R|^2 K^{00}(|\mathbf{R}|)\cos^2\gamma\, R^2\, dR\, d\Omega. \tag{3.18}$$

We can choose the origin of integration so that $\theta = \gamma$, and do the theta integration. But then we'll rewrite I_1 as if we hadn't done any integrals at all:

$$\int_{-1}^{1} \cos^2\gamma \;\; d\cos\gamma = \frac{2}{3} = \frac{1}{3}\int_{-1}^{1} d\cos\gamma$$

so that

$$I_1 = \frac{1}{3}\int R^2 A^2 K^{00}(R)\, d\mathbf{R}.$$

The second integral of the second order term will be simplified in a similar way.

$$I_2 = \int (\mathbf{A}\cdot\mathbf{R})(\mathbf{R}\cdot\nabla_u\Delta|_{\mathbf{r}}) K^{00}(R)\, R^2\, dR\, d\phi\, d\cos\theta.$$

We choose the origin of the solid angle integration so that the vector $\mathbf{A}$ lies along the z-axis ($\theta = \phi = 0$) and the vector $\mathbf{R}$ has $\phi = 0$ and an arbitrary θ. Then the vector $\nabla\Delta$ is defined by still arbitrary angles θ' and ϕ'. Thus the angle between $\mathbf{R}$ and $\nabla\Delta$ is γ where

$$\cos\gamma = \cos\theta\cos\theta' + \sin\theta\sin\theta'\cos\phi',$$

and we can write the integral as:

$$I_2 = \int (AR\cos\theta)(R|\nabla_u\Delta|\cos\gamma) K^{00}(R)\, R^2\, dR\, d\phi\, d\cos\theta.$$

We use the same trick to rewrite the angular integration:

$$\int \cos^2\theta\cos\theta'\, d\cos\theta = \left(\frac{2}{3}\right)\cos\theta' = \frac{1}{3}\cos\theta'\int d\cos\theta$$

and

$$I_2 = \int AR^2|\nabla\Delta| K^{00}(R)\frac{\cos\theta'}{3} d\mathbf{R}.$$

But θ' is the angle between $\mathbf{A}$ and $\nabla\Delta$, so

$$I_2 = \frac{1}{3}\int (\mathbf{A}\cdot\nabla\Delta)\, R^2 K^{00}(R)\, d\mathbf{R}.$$

Finally we turn our attention to the third second-order term.

$$\begin{aligned} I_3 &= \int d\mathbf{R} K^{00}(R) \frac{1}{2}\sum_{ij} R_i R_j \left.\frac{\partial^2\Delta}{\partial u_i \partial u_j}\right|_r \\ &= \frac{1}{2}\sum_{ij} \left.\frac{\partial^2\Delta}{\partial u_i \partial u_j}\right|_r \int_{-\infty}^{\infty} K^{00}(R)\, R_i R_j\, dR_x\, dR_y\, dR_z \end{aligned} \tag{3.19}$$

Now the terms in the sum for which $i \neq j$ will have integrals like

$$\int_{-\infty}^{\infty} R_x R_y\, K(|R|)\, dR_x$$

which are all zero, in this case because $K(|R|)$ is an even function of R_x, and R_x is odd. So the only contribution will come from the terms in the sum $i = j$, which together will contribute:

$$\begin{aligned} I_3 &= \frac{1}{2}\sum_i \left.\frac{\partial^2\Delta}{\partial u_i^2}\right|_r \int R_i^2\, K^{00}(R)\, d\mathbf{R} \\ &= \frac{1}{2}\sum_i \left.\frac{\partial^2\Delta}{\partial u_i^2}\right|_r \int (R\cos\theta_i)^2\, K^{00}(R)\, d\mathbf{R} \\ &= \frac{1}{2}\sum_i \left.\frac{\partial^2\Delta}{\partial u_i^2}\right|_r \frac{1}{3}\int R^2 K^{00}(R)\, d\mathbf{R}. \end{aligned} \tag{3.20}$$

The sum over the partial derivatives may now be done to yield:

$$I_3 = \frac{1}{6}\left.\nabla^2\Delta\right|_{\mathbf{r}} \int K^{00}(R) R^2\, d\mathbf{R}.$$

These integrations allow us to write the entire second order term as:

$$\frac{\lambda}{6}\left(\nabla + \frac{2ie}{\hbar}\mathbf{A}\right)^2 \Delta^*(\mathbf{r}) \int K^{00}(R) R^2\, d\mathbf{R},$$

and the approximate equation for the order parameter becomes:

$$\Delta^*(\mathbf{r}) = \lambda \left(\Delta^*(\mathbf{r}) \int K^{00}(R)\, d\mathbf{R} + \frac{1}{6} \left[\nabla + \frac{2ie}{\hbar} \mathbf{A} \right]^2 \Delta^*(\mathbf{r}) \int K^{00}(R) R^2\, d\mathbf{R} \right). \tag{3.21}$$

Abrikosov, Gorkov and Dzyaloshinski [29] have performed the kernel integrations in terms of parameters of the theory. From these results we obtain:

$$\int K^{00}(R)\, d\mathbf{R} = \frac{1}{\lambda} + \frac{m p_o}{2\pi^2} \left(\frac{T_c}{T} \right)^2 \left(\frac{T_c - T}{T_c} \right),$$

and

$$\int K^{00}(R) R^2\, d\mathbf{R} = \frac{7\zeta(3) v^2}{8\pi^2 T^2} \frac{m p_o}{2\pi^2}.$$

ζ is the Riemann zeta function, T_c is the critical temperature of the superconductor, and the Fermi velocity v is related to the Fermi energy: $E_f = \frac{1}{2} m v^2$. With a complex conjugation and the definition

$$\beta \equiv \frac{7\zeta(3)}{6\pi T_c^2} E_f,$$

the equation for the order parameter is seen to take the form of the linearized Ginsburg-Landau equation:

$$0 = \left(\frac{T_c - T}{T_c} \right) \frac{1}{\beta} \Delta + \frac{1}{4m} \left[\nabla - \frac{2ie\mathbf{A}}{\hbar} \right]^2 \Delta$$

or

$$0 = -\frac{\hbar^2}{\beta} \left(\frac{T_c - T}{T_c} \right) \Delta + \frac{1}{4m} \left[-i\hbar\nabla - 2eH \right]^2 \Delta.$$

Notice that it looks like a Schroedinger equation for a particle of twice the charge and mass of an electron, in a magnetic field. It is also very similar to the first order (in H) approximation which Abrikosov began with in his prediction of the vortex lattice in type-II superconductors [32]:

$$\left(\frac{i\nabla}{\kappa} + A \right)^2 \psi = \psi.$$

Once we substitute our expression for the magnetic potential $\mathbf{A} = xH\hat{y}$ into our linearized Ginsburg-Landau equation it may be rewritten as

$$\nabla^2\Delta(\mathbf{r}) - \frac{2ieH}{\hbar}x\frac{\partial\Delta}{\partial y} + \left(\alpha - 4x^2\left(\frac{eH}{\hbar}\right)^2\right)\Delta(\mathbf{r}) = 0,$$

where $\alpha = \frac{T_c - T}{T_c}\frac{4m}{\beta}$.

We'll follow Abrikosov's suggestion to try a solution of the form

$$\Delta(x,y) = \sum_{n=-\infty}^{\infty} c_n e^{ik_n y}\Psi_n(x).$$

(Recall that in our chosen gauge the momentum operator in the y-direction will commute with the "Hamiltonian" of our doubly charged and massed particle.) Since we expect to find a certain periodicity in the vortex lattice, we choose $k_n = \frac{2n\pi}{L_y}$, so that $\frac{L_y}{n}$ is the periodicity in the y-direction. Abrikosov's solution solves the differential equation subject to the condition that

$$\frac{\partial^2\Psi_n}{\partial x^2} = -\alpha\Psi_n(x) + \left(\frac{2eH}{\hbar}\right)^2(x - x_o)^2\Psi_n(x),$$

where $x_o = x_n = \frac{\hbar k_n}{2eH}$.

This equation for Ψ_n looks like the energy eigenvalue equation of a quantum mechanical harmonic oscillator, with the center of motion at x_n, a location that is different for each y-coordinate mode. As in the harmonic oscillator problem, the substitutions $u = \sqrt{\frac{2eH}{\hbar}}(x - x_n)$ and $\Psi_n(u) = e^{\frac{-u^2}{2}}H_\nu(u)$ yield Hermite's equation,

$$\frac{d^2H_\nu}{du^2} + 2\nu H_\nu - 2u\frac{dH_\nu}{du} = 0$$

where $2\nu = (\frac{\alpha\hbar}{2eH} - 1)$.

Hermite's equation has a series solution, however the boundary condition that the order parameter be finite, $\Psi(x \to \infty) \neq \infty$, requires that the series be terminated by making ν an integer ($\nu \to m$). This leaves us with the solutions

$$\Psi_{n,m}(x) = \exp\left(-\frac{2eH}{\hbar}\frac{(x - x_n)^2}{2}\right)H_m\left(\sqrt{\frac{2eH}{\hbar}}(x - x_n)\right).$$

In the analogy of the particle in a magnetic field, the index on the Hermite polynomial designates which Landau level the particle is in. Abrikosov chooses to use the zeroth order Hermite Polynomial, which is just 1. This gives us for the order parameter:

$$\Delta(x,y) = \sum_{n=-\infty}^{\infty} c_n e^{ik_n y} \exp\left(-\frac{eB}{\hbar}(x-x_n)^2\right),$$

with $k_n = \frac{2n\pi}{L_y}$ and $x_n = \frac{\hbar k_n}{2eH}$. There are several choices for the coefficients c_n, which will determine the precise periodicity of the vortex lattice. It is necessary that $c_n = c_{n+N}$, with N integer, for the order parameter to be periodic in x as well as y. Abrikosov chose $N = 1$, which yields a square vortex lattice. A slightly different choice for the coefficients is necessary to obtain the triangular lattice, however nothing else about the order parameter changes with the lattice shape.

Now this expression for the order parameter can be used in the Gorkov expression for the Green's function,

$$G_{(\mathbf{r},\mathbf{r}')} = G^{0}_{(\mathbf{r},\mathbf{r}')} - \int d\mathbf{l} \int d\mathbf{l}'\, G^{0}_{(\mathbf{r},\mathbf{l})}\, \Delta(\mathbf{l})\, G^{0}_{-\omega(\mathbf{l},\mathbf{l}')}\, \Delta^*(\mathbf{l}')\, G_{(\mathbf{l}',\mathbf{r}')}.$$

Recalling our semi-classical approximation that a magnetic field changes the Green's function by a phase:

$$G^{0}_{(\mathbf{r},\mathbf{r}')} = e^{\varphi(\mathbf{r},\mathbf{r}')} G^{00}_{(\mathbf{r}-\mathbf{r}')},$$

with

$$\varphi(\mathbf{r},\mathbf{r}') = \frac{ieB}{\hbar}\frac{(r_x + r'_x)}{2}(r'_y - r_y),$$

this yields

$$\begin{aligned} G_{(\mathbf{r},\mathbf{r}')} &= e^{\varphi(\mathbf{r},\mathbf{r}')} G^{00}_{(\mathbf{r}-\mathbf{r}')} \\ &- \int d\mathbf{l} \int d\mathbf{l}'\, e^{\frac{ieB}{\hbar}} \left[\frac{(r_x + l_x)}{2}(l_y - r_y) + \frac{(l_x + l'_x)}{2}(l'_y - l_y)\right] G^{00}_{(\mathbf{r}-\mathbf{l})} G^{00}_{(\mathbf{l}-\mathbf{l}')} \\ &\sum_{n,m=-\infty}^{\infty} c_n c_m^* e^{ik_n l_y} e^{-ik_m l'_y} \exp\left(\left[-\frac{eB}{\hbar}\right]\left[(l_x - x_n)^2 + (l'_x - x_m)^2\right]\right) G_{(\mathbf{l}',\mathbf{r}')} \end{aligned} \tag{3.22}$$

Brandt uses Eilenberger's Green's function [93], which differs from the Gorkov one we've been using by a phase factor. A switch to this Green's function allows Gorkov's equation to be written in terms of Green's functions and a potential which depends only on the variables of integration.

$$G_{(\mathbf{r},\mathbf{r}')} = G^{00}_{(\mathbf{r}-\mathbf{r}')} - \int d\mathbf{l} \int d\mathbf{l}' \, G^{00}_{(\mathbf{r}-\mathbf{l})} V(l,l') G^{00}_{-\omega(\mathbf{l}-\mathbf{l}')} G r l' r' \tag{3.23}$$

where

$$V(l,l') = \Delta(\mathbf{l},\mathbf{l}') e^{i(2?)\varphi(\mathbf{l},\mathbf{l}')}$$

and Δ and φ are still defined as above.

A Fourier transform to momenta conjugate to the sum $(K, \frac{1}{2}(\mathbf{r}+\mathbf{r}')$ and difference $(p, \mathbf{r}-\mathbf{r}')$ coordinates yields the Green's function $G_{(\mathbf{p},\mathbf{K})}$ and its equation

$$G_{(\mathbf{p}-\frac{\mathbf{L}}{\mathbf{2}},-\mathbf{L})} = \delta_{L,0} G^{00}_{(\mathbf{p})} - G^{00}_{(\mathbf{p}-\mathbf{L})} \sum_{L'} G_{(\mathbf{p}-\frac{\mathbf{1}}{\mathbf{2}}(\mathbf{L}+\mathbf{L}"),-(\mathbf{L}+\mathbf{L}'))} \times \frac{1}{(2\pi)^3} \int d\mathbf{p}' V(\mathbf{p}',\mathbf{L}') G^{00}_{-\omega(\mathbf{p}-\mathbf{p}'-\mathbf{L}-\frac{\mathbf{L}'}{\mathbf{2}})}. \tag{3.24}$$

The vector $\mathbf{L} = \mathbf{n}\sqrt{2\pi}/\Lambda$ (where $\mathbf{n}$ is now a vector, with integer components, and $\Lambda = \sqrt{\frac{1}{2eB\hbar}}$) is a reciprocal vector to the lattice of flux lines. $G^{00}_{(\mathbf{p})}$ is the free electron Green's function in zero field, so depends only on the momenta conjugate to the difference coordinate. As usual

$$G^{00}_{(\mathbf{p})} = \frac{1}{i\omega_n - (\frac{p^2}{2m} - \mu)} \tag{3.25}$$

$$G^{00}_{-\omega(\mathbf{p})} = \frac{-1}{i\omega_n + (\frac{p^2}{2m} - \mu)} \tag{3.26}$$

The potential due to the order parameter in momenta coordinates is

$$V(\mathbf{p},\mathbf{L}) = 2(2\pi)^2 \delta(p_z) \langle \Delta^2 \rangle_{orb} \Lambda^2 \exp[(p_x^2 + p_y^2)] \exp[i\Lambda^2(-p_x L_y + p_y L_x + \frac{L_x L_y}{2})] \tag{3.27}$$

By taking $\mathbf{K} = 0$ we can find a spatial average of the Green's function, which still takes into account the effect of the spatial variation of the phase of the order parameter due to the flux lattice. This is appropriate when the magnitude of the order parameter is not changing drastically, that is, near H_{c2} when flux penetration is dense. In the above equation this implies $\mathbf{L} = 0$, in which case the $\mathbf{L}' = 0$ term in the sum is the dominant term. This finally yields

$$G_{(\mathbf{p},\mathbf{0})} = \left(\frac{1}{G^{00}_{(\mathbf{p})}} - \Sigma(\mathbf{p}, 0, \omega_n) \right)^{-1}. \tag{3.28}$$

This takes the form of Dyson's equation, with a self energy which modifies the Green's function. In this case the self energy is

$$\Sigma(\mathbf{p}, 0, \omega_n) = \frac{-1}{(2\pi)^3} \int d\mathbf{p}' V(\mathbf{p}', 0) G^{00}_{-\omega(\mathbf{p}-\mathbf{p}')}$$

where

$$V(\mathbf{p}', 0) = 2(2\pi)^2 \left\langle \Delta^2 \right\rangle_{orbital\,average} \Lambda^2 \delta(p'_z) e^{-\Lambda^2(p'^2_x + p'^2_y)},$$

and $\Lambda = \sqrt{\frac{1}{2eB\hbar}}$.

3.4.3. The Superconducting Self-Energy in the Vortex State

In order to use the self-energy we have just calculated we need to simplify it, and examine its properties in the complex plane.

The Green's function contains the term $(\mathbf{p} - \mathbf{p}')^2$, which may be written $\mathbf{p}^2 + \mathbf{p}'^2 - 2\mathbf{p} \cdot \mathbf{p}'$. Once the delta function integration in the z-component is carried out, $\mathbf{p}'$ has only x and y coordinates. With a change to polar coordinates using the substitutions $p'_x = t\cos\phi$ and $p'_y = t\sin\phi$ the self energy becomes

$$\Sigma(\mathbf{p}, 0, \omega_n) = \frac{\Delta^2 \Lambda^2}{\pi} \int_0^{2\pi} \int_0^{\infty} \frac{t\, dt\, d(\phi - \phi') e^{-\Lambda^2 t^2}}{i\omega_n + \frac{p^2}{2m} - \mu + \frac{t^2}{2m} - \frac{2tp}{2m} \sin\theta \cos(\phi' - \phi)}.$$

Now t may be replaced with a unitless variable using the substitution $s = t/\sqrt{2m\mu}$ or $s = t/mv_f$ with $\mu = \frac{1}{2}mv_f^2$. The Gaussian term then becomes $\exp(-(\mu/\hbar\omega_c)s^2)$. Because the chemical potential is much larger than the cyclotron frequency (energy), the largest contribution to the integral will be near $s = 0$, and the integrand can be expanded around that point. The radial and angular integrations can then be done term by term. The expansion is best done by computer, but the result is that the nth-order term contains $\cos\phi$ raised to the power of n-1. Thus terms with even n have an odd power of cosine, which integrates to zero. The odd terms contain the integral

$$\int_0^{2\pi} \cos^{2m}\phi \, d\phi = \frac{2\pi(2m)!}{2^{2m}(m!)^2},$$

with $2m = n - 1$ (an even number), as well as the radial integral which looks like

$$\int_0^{\infty} x^{2n+1} e^{-ax^2} \, dx = \frac{n!}{2a^{n+1}}.$$

The result is the sum:

$$\Sigma(\mathbf{p}, 0, \omega_n) = \frac{\Delta^2}{a} \sum_{m=0}^{\infty} \frac{(2m)!}{m!} \left(\frac{v_f \sin\theta}{2a\Lambda} \right)^{2m} \tag{3.29}$$

where $a = i\omega_n + p^2/2m - \mu$, and we've assumed that the relevant momentum is near the Fermi energy so $p^2 = 2m_b\mu$. This sum is equivalent to the integral Brandt uses for the self energy,

$$\Sigma(\mathbf{p}, 0, \omega_n) = \frac{1}{\sqrt{\pi}} \frac{\Delta^2\Lambda}{v_f \sin\theta} \int_{-\infty}^{\infty} \frac{dt \, e^{-t^2}}{z - t} \tag{3.30}$$

with $z = a\Lambda/v_f \sin\theta$, as can be seen by a series expansion of this integral. For future reference, we'll note that this is a complex expression ($\zeta_n = i\omega_n + \mu = i\tau_n$), with the imaginary part of the self energy being:

$$\Im\left(\Sigma(\mathbf{p}, 0, \omega_n)\right) = \frac{-1}{\sqrt{\pi}} \frac{\Delta^2\Lambda^2}{v_f^2 \sin^2\theta} \int_{-\infty}^{\infty} \frac{dt \, e^{-t^2} \omega_n}{\left(\frac{\Lambda(p^2/2m - \mu)}{v_f \sin\theta} - t \right)^2 + \left(\frac{\Lambda}{v_f \sin\theta} \omega_n \right)^2}, \tag{3.31}$$

which has the opposite sign as the sign of ω_n. Whereas the real part is:

$$\Re\left(\Sigma(\mathbf{p},0,\omega_n)\right) = \frac{1}{\sqrt{\pi}}\frac{\Delta^2\Lambda}{v_f\sin\theta}\int_{-\infty}^{\infty}\frac{dt\, e^{-t^2}\left(-t+\frac{\Lambda(p^2/2m-\mu)}{v_f\sin\theta}\right)}{\left(\frac{\Lambda(p^2/2m-\mu)}{v_f\sin\theta}-t\right)^2+\left(\frac{\Lambda}{v_f\sin\theta}\omega_n\right)^2}. \tag{3.32}$$

4. THE GREEN'S MATRIX FOR A HEAVY FERMION SUPERCONDUCTOR

4.1. Superconducting Self Energy in the Green's Matrix

We recall that the heavy fermion Green's matrix is:

$$G = \begin{pmatrix} G_{ff}(\zeta_n) & G_{fc}(\zeta_n) \\ G_{cf}(\zeta_n) & G_{cc}(\zeta_n) \end{pmatrix} \tag{4.1}$$

with the matrix elements

$$\begin{aligned} G_{ff}(\zeta_n) &= \left(\zeta_n - (E_f + \lambda - mh) - \frac{V^2 z^2}{\zeta_n - \mathcal{E}_{km}}\right)^{-1} \\ &= \frac{\zeta_n - \mathcal{E}_{km}}{(\zeta_n - \mathcal{E}_{km})(\zeta_n - (E_f + \lambda - mh)) - V^2 z^2} \end{aligned} \tag{4.2}$$

$$G_{fc}(\zeta_n) = G_{cf} = \frac{Vz}{(\zeta_n - \mathcal{E}_{km})(\zeta_n - (E_f + \lambda - mh)) - V^2 z^2} \tag{4.3}$$

$$\begin{aligned} G_{cc}(\zeta_n) &= \left(\zeta_n - \mathcal{E}_{km} - \frac{V^2 z^2}{\zeta_n - (E_f + \lambda - mh)}\right)^{-1} \\ &= \frac{\zeta_n - (E_f + \lambda - mh)}{(\zeta_n - \mathcal{E}_{km})(\zeta_n - (E_f + \lambda - mh)) - V^2 z^2}. \end{aligned} \tag{4.4}$$

This result derives from the Green's function for non-interacting conduction band electrons, $(\zeta_n - \mathcal{E}_{km})^{-1}$, and this term (or its reciprocal) appears in all the matrix elements. We have seen in the previous chapter (equation 3.28) that the presence of a superconducting vortex lattice alters the Green's function by the insertion of a self energy:

$$(\zeta_n - \mathcal{E}(\mathbf{p}) - \Sigma)^{-1}$$

$$\Sigma(\mathbf{p}, 0, \zeta_n) = \frac{1}{\sqrt{\pi}} \frac{\Delta^2 \Lambda^2}{v_f \sin\theta} \int_{-\infty}^{\infty} \frac{dt\, e^{-t^2}}{z - t}$$

Here we consider the implications of inserting this superconducting self-energy into all the terms in the Green's matrix which look like the conduction band Green's function. We will change the momentum variable in the self-energy, $\mathbf{p}$, to $\hbar\mathbf{k}$ so it

will be consistent with the choice for the heavy fermion system, and to free up p to become a Landau level index.

The $\sin(\theta)$ in the superconducting self-energy measures the angle between the velocity of the electron and the magnetic field. However, a de Haas-van Alphen experiment observes only electrons at the Fermi surface. In a superconductor only electrons with momentum perpendicular to the vortex lattice (and magnetic field) have a Fermi surface, so for our purposes the $\sin(\theta)$ term reduces to 1.

Another modification of the Green's functions is due to the magnetic field. The free particle states, $\mathcal{E}_{km}$ will be replaced by Landau levels,

$$\mathcal{E}(p, k_z, m) = \frac{k_z^2}{2m_b} + \omega_c(p + \frac{1}{2}) - mh. \tag{4.5}$$

(The f-orbitals are so localized that Landau orbits are not applicable. The only interaction they have with the magnetic field is due to their spin state, m.)

Replacing the conduction band electrons with superconducting electrons in Landau levels yeilds the following Green's matrix elements:

$$\begin{aligned} G_{ff}(\zeta_n) &= \left(\zeta_n - \tilde{E}_f - \frac{V^2 z^2}{\zeta_n - \tilde{E}_{pkm}}\right)^{-1} \\ &= \frac{\zeta_n - \tilde{E}_{pkm}}{(\zeta_n - \tilde{E}_{pkm})(\zeta_n - \tilde{E}_f) - V^2 z^2} \qquad (4.6) \\ G_{fc}(\zeta_n) = G_{cf} &= \frac{Vz}{(\zeta_n - \tilde{E}_{pkm})(\zeta_n - \tilde{E}_f) - V^2 z^2} \qquad (4.7) \\ G_{cc}(\zeta_n) &= \left(\zeta_n - \tilde{E}_{km} - \frac{V^2 z^2}{\zeta_n - \tilde{E}_f}\right)^{-1} \\ &= \frac{\zeta_n - \tilde{E}_f}{(\zeta_n - \tilde{E}_{km})(\zeta_n - \tilde{E}_f) - V^2 z^2}, \qquad (4.8) \end{aligned}$$

where

$$\tilde{E}_f = E_f + \lambda - mh, \tag{4.9}$$

and

$$\tilde{E}_{pkm} = \frac{k_z^2}{2m_b} + \omega_c(p + \frac{1}{2}) - mh + \Sigma. \tag{4.10}$$

5. DE HAAS-VAN ALPHEN AND THE EXTENDED LIFSHITZ-KOSEVICH METHOD

5.1. A Qualitative Explanation of the de Haas-van Alphen Effect

Classical free electrons in a magnetic field travel in circular or spiral orbits, which could be characterized by the momentum parallel to the field and the circular motion perpendicular to it. Quantized electrons in a magnetic field also have energy levels characterized by these two quantities. Their energies are given by $E = \frac{\hbar^2 k_z^2}{2m_o} + \frac{eB\hbar}{m_o}(p + \frac{1}{2})$. The momentum parallel to the field is given by k_z (nearly continuous), and the quantum number p designates a Landau level. The Landau levels are represented by concentric cylinders in momentum space indexed by p.

For free electrons any surface of constant energy, e.g. the Fermi surface, is a sphere in momentum space. The occupied states are those whose Landau level, p, and parallel momentum, k_z are such that the total energy of the state is less than the Fermi energy.

The energy of a Landau level (the radius of the cylinder) is proportional to the field. So as the field is increased, the cylinders grow, and the number of states (allowed k_z values) in any particular level decreases, and then abruptly goes to zero when that Landau level crosses the Fermi energy. The total energy of all occupied states will change abruptly with this crossing, then change smoothly again as the next Landau level increases its radius, until it also crosses the Fermi energy. These crossings occur at equal intervals in $1/H$ [1], with a frequency determined by the

---

[1]The Landau levels are equally spaced at any given field, but the larger the field the greater the spacing. So as the field increases, the frequency of crossings decreases.

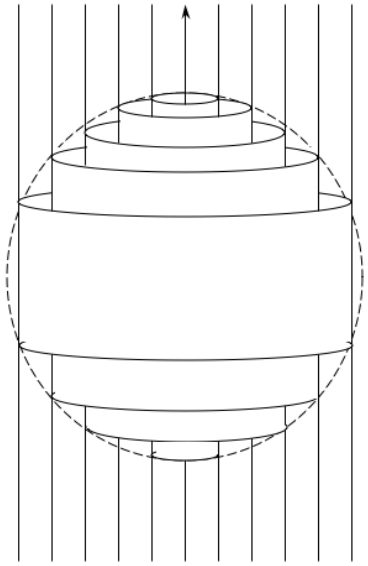

FIGURE 5.1. Landau levels for electrons inside the Fermi surface

largest (extremal[2]) cross sectional area of the Fermi surface, $A(\theta, \phi)$.[3] These oscillations in energy (and therefore thermodynamic potential) lead directly to oscillations in the magnetization of the sample. These are known as de Haas-van Alphen os-

---

[2]Just as the largest cross sectional area of a Fermi surface causes oscillations as a cylinder leaves the occupied region entirely, if the Fermi surface has a minima, this will also cause oscillations as the cylinder becomes partially unoccupied.

[3]Since the spacing between levels scales linearly with field, a larger radius Fermi surface will see more levels cross for the same change in field. Imagine a rubber band with Landau levels marked on it every centimeter. Place it next to a ruler, and stretch it til it doubles its length. The two centimeter mark on the ruler will only see one level pass it ($p = 1$). But the six centimeter mark will see three levels pass it ($p = 4, 5, \text{and } 6$).

cillations, observed by de Haas and van Alphen [94] and predicted by Landau [95] almost concurrently. The dependence of the frequency in $\frac{1}{H}$ on the extremal cross sectional area of the Fermi surface allows the Fermi surface to be mapped out by changing the orientation of the field. In fact, its reliability and versatility in this capacity helped establish the concept of a Fermi surface, and it has been in wide use for this purpose since the 1960's.

These oscillations are, of course, observed not in free electrons but in metals. Using a Fermi liquid model, nearly independent quasiparticles replace the electrons. The number of electrons in partially filled bands (i.e. those which are statistically relevant) is equal to the number of quasiparticles. The energy spectrum of a quasiparticle is modified from that of a free electron by interactions with the lattice and every other conceivable interaction. This leads to non-spherical Fermi surfaces in quasi-momentum space, which reflect the symmetry of the lattice. The Fermi surface of a metal is one of its most characteristic features, defining the behavior of the electrons and thus many of the macroscopic physical properties. (A non-spherical surface will change the amplitude of the oscillations. For example, a cylindrical Fermi surface aligned with the field will have more states affected when a Landau level crosses it, and a larger amplitude.)

Several effects can reduce the amplitude of the dHvA oscillations. Generally this is the result of "phase smearing". If a Landau level is not uniform in its approach to the Fermi surface, a superposition of oscillations which are slightly out of phase reduces the amplitude. One example is Zeeman splitting of the energy levels due to the spin of the electrons. The interaction of the spin with the magnetic field results in a Zeeman splitting of $\frac{1}{2}g\frac{e\hbar}{m_o c}B$. The spin-up and spin-down sheets will pass through the Fermi energy separately, and the sum of the two phase shifted oscillations will be reduced from the amplitude of the single unsplit sheet. (Because

$\sin(x+y)+\sin(x-y) = 2\cos(y)\sin(x)$.) (This is not the only effect of Zeeman splitting, as will be seen in the field dependence of the effective mass in a heavy fermion material.)

A finite temperature will have a somewhat similar effect, though the form of the amplitude reduction is slightly different. At finite temperatures the Fermi surface is no longer sharp. Thus the migration of quasiparticles out of a Landau level no longer occurs simultaneously as it passes a single energy value. Phase shifted migrations reduce the amplitude, however in this case the effective mass is an important parameter in the amplitude reduction. The temperature dependence of the amplitude is used in this way as one of the most reliable measures of electron (cyclotron) effective mass.

Electron impurity scattering, and field or sample inhomogeneity result in an exponential reduction factor, known as the Dingle factor.

The canonical Lifshitz-Kosevitch [96] result describing the thermodynamic potential for dHvA oscillations consists of these several amplitude reduction factors multiplied by the basic oscillations:

$$\Omega_{osc} = \left(\frac{e}{2\pi c\hbar}\right)^{\frac{3}{2}} \frac{e\hbar B^{\frac{5}{2}}}{m^*\pi^2} \left|\frac{\partial A_i}{\partial k_z^2}\right|^{-\frac{1}{2}} \sum_{r=1}^{\infty} r^{-5/2} R_D R_T R_\sigma \cos\left[2\pi r\left(\frac{F_i}{B}-\gamma\right)\pm\frac{\pi}{4}\right], \quad (5.1)$$

with the Dingle factor

$$R_D = e^{\frac{-r\pi}{\omega_c\tau}},$$

the thermal damping factor

$$R_T = \frac{2\pi^2 r k_B T}{\hbar\omega_c \sinh(\frac{2\pi^2 r k_B T}{\hbar\omega_c})},$$

(recall the cyclotron frequency contains the effective mass) and the Zeeman spin splitting factor

$$R_\sigma = \cos\left(\frac{r\pi g m^*}{2m_e}\right).$$

The frequency is given by

$$F_i(\theta, \phi) = \frac{\hbar A_i(\theta, \phi)}{2\pi e}.$$

The index i is included to allow for multiple sheets of the Fermi surface, which are often seen in real metals.

(This expression is only the oscillatory part of the thermodynamic potential. Constant terms have been dropped.) The magnetization is the derivative of this potential with respect to the magnetic field, and has essentially the same form.

5.2. Extended Lifshitz-Kosevitch

The Lifshitz-Kosevitch result is quasi-classical. It has no method for dealing with the many-body effects we are interested in here. By recasting the problem in terms of Green's functions, we will see a very similar form of the thermodynamic potential, however the role of complex self energies will be made explicit.

Wasserman and Springford [92] have a detailed derivation of the thermodynamic potential as the trace of the natural log of the Green's function:

$$\Omega = -T \sum_n \mathrm{Tr} \log(-G^{-1}(\zeta_n)). \tag{5.2}$$

The trace arises from a sum over states and is over all the different ways to designate a state. The Green's matrix is diagonal in k_z, p, and m (i.e. it is not a function of k_z and k_z', p and p' or m and m') so those parts of the trace appear merely as sums or integrals over m, p and k_z. The trace over the f orbitals and conduction band states appears in the usual way for the non-diagonal matrix, $\log(-G^{-1})$. The order of operation of the trace and the logarithm is not interchangable, but an identity from linear algebra specifies how to take the trace of a log of a matrix.

$$\mathrm{Tr}(\log \mathbf{A}) = \log(\det(\mathbf{A})) \tag{5.3}$$

so

$$\Omega_{osc} = -T \sum_n \mathrm{Tr}\ \log(-G^{-1}(\zeta_n)) = -T\mathrm{Tr}\ \log(\det(-G^{-1}_{\alpha\beta}(\zeta_n)), \tag{5.4}$$

where now the trace that remains is only over the different states that an f or c electron could be in...k_z, p, and m, ultimately.

This yields for our case of an f-c Greens matrix, the thermodynamic potential:

$$\Omega = -T\,\frac{L^3 m_b \omega_c}{2\pi h} \int_{-\infty}^{\infty} dk_z \sum_{p=0}^{\infty} \sum_{m=-J}^{J} \sum_n \ln[-(G_{cc}G_{ff} - G_{fc}^2)^{-1}].$$

5.3. Previous Results Using the Extended Lifshitz-Kosevitch Method

Wasserman and Springford have applied the extended Lifshitz-Kosevitch method to the de Haas-van Alphen experiment in a variety of cases. The method reproduces the Dingle reduction factor for a self-energy due to non-magnetic impurity scattering. Likewise it reproduces the well-known Stoner enhancement in the spin-splitting amplitude reduction due to electron correlations in the screened Hartree-Fock approximation. It captures the non-quasiparticle behavior of, e.g. mercury, at high fields due to electron-phonon coupling, as also predicted by Englesberg and Simpson. The many-body interactions in a superconductor are successfully taken into account, and lead to a new amplitude reduction factor in type-II superconductors. In this case the result is equivalent to that due to Maki [97]. These consistencies with other theories are reassuring. However one significant extension to behavior not previously accounted for comes in the case of heavy fermion materials. Rasul's path integral formulation of dHvA [98] is capable of explaining the enhanced effective mass of heavy fermion materials. However, no field dependence of the mass is obtainable in this way: the method only applies at zero field. Extended Lifshitz-

Kosevich reproduces Rasul's result, but also explains the reduction in this enhanced mass with increased field. The fit to the experimental data is quite good.

The technique has proven itself to be an accurate and unified approach to the de Haas-van Alphen experiment.

6. RESULTS

6.1. Calculation of m* from the HFSC Green's Matrix

We have seen previously that the Green's matrix for a heavy fermion superconductor is:

$$G = \begin{pmatrix} G_{ff}(\zeta_n) & G_{fc}(\zeta_n) \\ G_{cf}(\zeta_n) & G_{cc}(\zeta_n) \end{pmatrix}, \tag{6.1}$$

with the elements given by:

$$\begin{aligned} G_{ff}(\zeta_n) &= \left(\zeta_n - \tilde{E}_f - \frac{V^2 z^2}{\zeta_n - \tilde{E}_{pkm}}\right)^{-1} \\ &= \frac{\zeta_n - \tilde{E}_{pkm}}{(\zeta_n - \tilde{E}_{pkm})(\zeta_n - \tilde{E}_f) - V^2 z^2} \end{aligned} \tag{6.2}$$

$$G_{fc}(\zeta_n) = G_{cf} = \frac{Vz}{(\zeta_n - \tilde{E}_{pkm})(\zeta_n - \tilde{E}_f) - V^2 z^2} \tag{6.3}$$

$$\begin{aligned} G_{cc}(\zeta_n) &= \left(\zeta_n - \tilde{E}_{km} - \frac{V^2 z^2}{\zeta_n - \tilde{E}_f}\right)^{-1} \\ &= \frac{\zeta_n - \tilde{E}_f}{(\zeta_n - \tilde{E}_{km})(\zeta_n - \tilde{E}_f) - V^2 z^2}, \end{aligned} \tag{6.4}$$

where

$$\tilde{E}_f = E_f + \lambda - mh, \tag{6.5}$$

and

$$\tilde{E}_{pkm} = \frac{k_z^2}{2m_b} + \omega_c(p + \frac{1}{2}) - mh + \Sigma. \tag{6.6}$$

We have also seen that the grand thermodynamic potential for a de Haas-van Alphen experiment is given by

$$\Omega = -T \operatorname{Tr} \sum_n \ln[-G^{-1}(\zeta_n)].$$

The trace here is a sum over states, so it includes both the trace of the matrix and a sum over the quantum numbers k_z, p, and m. The trace of the matrix becomes a determinant inside the logarithm, as indicated in the previous chapter (Equation 5.3). Since k_z is continuous its sum becomes an integral with a factor of $L/2\pi$. A degeneracy factor is necessary to account for the Landau levels, which have many states for the same quantum number. This degeneracy is $g = \frac{L_x L_y m_b \omega_c}{h}$, so the potential becomes:

$$\Omega = -T\,\frac{L^3 m_b \omega_c}{2\pi h}\int_{-\infty}^{\infty} dk_z \sum_{p=0}^{\infty}\sum_{m=-J}^{J}\sum_{n}\ln[-(G_{cc}G_{ff} - G_{fc}^2)^{-1}].$$

The degeneracy factor is given here with the correct factors of $\hbar$ to avoid confusion. However in terms which obviously have units of energy, the $\hbar$ is dropped for brevity. In the final result this will be corrected and all $\hbar$'s restored.

The determinant of the matrix is not difficult to perform:

$$-(G_{cc}G_{ff} - G_{fc}^2)^{-1} = (\zeta_n - \tilde{E}_f)\left(\frac{V^2 z^2}{\zeta_n - \tilde{E}_f} - (\zeta_n - \tilde{E}_{pkm})\right),$$

and the logarithm becomes

$$\ln\left[-(G_{cc}G_{ff} - G_{fc}^2)^{-1}\right] = \ln(\zeta_n - \tilde{E}_f) + \ln\left(\frac{V^2 z^2}{\zeta_n - \tilde{E}_f} - (\zeta_n - \tilde{E}_{pkm})\right).$$

Since the f-electrons are very localized, they do not participate in the de Haas-van Alphen oscillations. Thus the first term in the logarithm must be a constant and not a contribution to the oscillatory part of the thermodynamic potential. We subsequently neglect it. The second term we rewrite using an integral representation for the natural logarithm. For x and y real numbers:

$$\ln(x+iy) = \lim_{b\to 0^+}\begin{cases} -\int_{b-i\infty}^{b}\frac{ds}{s}e^{-s(x+iy)} & \text{for } y>0 \\ \int_{b}^{b+i\infty}\frac{ds}{s}e^{-s(x+iy)} & \text{for } y<0 \end{cases}$$

The real and imaginary parts of the argument of our logarithm are:

$$x = \Re\left(\frac{V^2 z^2}{\zeta_n - \tilde{E}_f} - (\zeta_n - \tilde{E}_{pkm})\right) = \tilde{E}_{pkm} - \mu + \frac{V^2 z^2(\mu - \tilde{E}_f)}{\omega_n^2 + (\tilde{E}_f - \mu)^2} + \Re(\Sigma),$$

and

$$y = \Im\left(\frac{V^2 z^2}{\zeta_n - \tilde{E}_f} - (\zeta_n - \tilde{E}_{pkm})\right) = -\omega_n - \frac{\omega_n V^2 z^2}{\omega_n^2 + (\tilde{E}_f - \mu)^2} + \Im(\Sigma).$$

Notice that the imaginary part has the opposite sign of ω_n. This means that the second integral representation applies for all positive values of ω_n, and the first for all negative values, and we can write the potential as:

$$\Omega = -T\,\frac{L^3 m_b \omega_c}{2\pi h}\int_{-\infty}^{\infty} dk_z \sum_{p,m} \lim_{b\to 0^+}\left[\sum_{n=0}^{\infty}\int_b^{b+i\infty}\frac{ds}{s}e^{-s\left(\tilde{E}_{pkm}-\zeta_n+\frac{V^2 z^2}{\zeta_n-\tilde{E}_f}\right)}\right.$$
$$\left. - \sum_{n=-\infty}^{0}\int_{b-i\infty}^{b}\frac{ds}{s}e^{-s\left(\tilde{E}_{pkm}-\zeta_n+\frac{V^2 z^2}{\zeta_n-\tilde{E}_f}\right)}\right].$$

Now we turn our attention to the integral over k_z. The only term which contains this variable is $\tilde{E}_{pkm} = \frac{k_z^2}{2m_b} + \omega_c(p+\frac{1}{2}) - mh + \Sigma$. Neglecting the k_z-dependence in the superconducting self energy, the integral looks like:

$$\int_{-\infty}^{\infty} dk_z e^{-sk_z^2/2m}.$$

Since s is complex, the method of steepest descents is necessary to evaluate this Gaussian integral. We generalize k_z to a complex variable $z = |z|e^{i\theta}$, and let s be represented by $|s|e^{i\phi}$. The integral becomes

$$\int_{-\infty}^{\infty} dz e^{|s|u} e^{i|s|v}$$

where

$$u = -|z|^2\cos(\phi+2\theta)/2m, \text{ and } v = -|z|^2\sin(\phi+2\theta)/2m.$$

The function u has a saddle point in the complex plane at $|z| = 0$. We deform the contour which originally ran along the real-axis to one along which the function v is constant, that is, the integrand is not oscillating. By Cauchy-Riemann conditions, this is the contour of steepest descent of the function u as we move away from the

saddle point. This path occurs for $\theta = -\phi/2$ or $\pi - \phi/2$. In other words we rotate our original path from $-\infty$ to ∞ by $-\phi/2$. Along the new path, the complex number z is defined by $z = te^{-i\phi/2}$, with t a real number ranging from $-\infty$ to ∞, and the integral along this path is then

$$\int_{t=-\infty}^{t=\infty} e^{-|s|t^2/2m} dt\, e^{-i\phi/2} = e^{-i\phi/2}\sqrt{\frac{m}{|s|}}\sqrt{2\pi}.$$

Recall that the variable ϕ represents the phase of the variable s which is part of the previous contour integration. It runs along the imaginary axis, from $-\infty$ to ∞, so its phase is $\pi/2$ when the imaginary part of s is positive, and $-\pi/2$ when negative. This leaves the present integral with the value

$$e^{\mp i\pi/4}\sqrt{\frac{2m\pi}{|s|}}.$$

This is also a convenient time to perform the sum over the Landau-level index, p. This variable also appears due to $\tilde{E}_{pkm}$, and we have a sum which appears as:

$$\sum_{p=0}^{\infty} e^{-s\omega_c(p+1/2)}.$$

This is recognized as a binomial series:

$$\sum_{p=0}^{\infty} e^{-s\omega_c(p+1/2)} = e^{-s\omega_c/2}\sum_{p=0}^{\infty}\left(e^{-s\omega_c}\right)^p = e^{-s\omega_c/2}\left(1-e^{-s\omega_c}\right)^{-1} = \left[e^{s\omega_c/2}\left(1-e^{-s\omega_c}\right)\right]^{-1}$$
$$= \left[2\sinh\left(\frac{s\omega_c}{2}\right)\right]^{-1}.$$

With these results, the thermodynamic potential becomes:

$$\Omega = -T\,\frac{L^3 m_b \omega_c}{2\pi h}\lim_{b\to 0^+}\sum_{m=-J}^{J}$$
$$\left[\sum_{n=0}^{\infty}\int_b^{b+i\infty}\frac{ds}{s}\sqrt{\frac{2m\pi}{|s|}}e^{-i\pi/4}\left[2\sinh\frac{s\omega_c}{2}\right]^{-1} e^{-s\left(-mh+\langle\Sigma\rangle_{ext.or.}-\zeta_n+\frac{V^2 z^2}{\zeta_n-\tilde{E}_f}\right)}\right.$$
$$\left. -\sum_{n=-\infty}^{0}\int_{b-i\infty}^{b}\frac{ds}{s}\sqrt{\frac{2m\pi}{|s|}}e^{i\pi/4}\left[2\sinh\frac{s\omega_c}{2}\right]^{-1} e^{-s\left(-mh+\langle\Sigma\rangle_{ext.or.}-\zeta_n+\frac{V^2 z^2}{\zeta_n-\tilde{E}_f}\right)}\right]. \quad (6.7)$$

In the sum and integral above we ignored the energy dependence of the superconducting self energy. This may be justified by the $\Lambda = \sqrt{\frac{c}{2eB\hbar}}$ in this self energy, which makes these higher order terms (in one over the magnetic field). Instead, we take the average of the self energy over the extremal orbit on the Fermi surface. For a spherical Fermi surface and cylindrical Landau levels, this extremal orbit corresponds to $k_z = 0$, which is the location of the maximum of the Gaussian in the previous integral.

To perform the contour integration in s, we note that the inverse of the hyperbolic sine has poles where

$$e^{s\omega_c/2} = e^{-s\omega_c/2} \text{ or } \frac{s\omega_c}{2} = i\pi r \ (r = \text{integer}).$$

All the poles have the same character, i.e. they are simple poles, as can be seen by the expansion of $2(\sinh x)^{-1}$ around $x = 0$:

$$\left[e^x - e^{-x}\right]^{-1} = \left[\left(1 + x + \frac{x^2}{2!} + \frac{x^3}{3!}...\right) - \left(1 - x + \frac{x^2}{2!} - \frac{x^3}{3!}...\right)\right]^{-1}$$
$$= \left[2\left(x + \frac{x^3}{3!} + ...\right)\right]^{-1} = \frac{1}{2x}\left(1 + \frac{x^2}{3!} + ...\right)^{-1} \approx \frac{1}{2x}\left(1 - \frac{x^2}{3!} - ...\right).$$

At $s = 0$ the integrand has a higher than first order pole because of the terms other than the hyperbolic sine. Each of the other poles of the hyperbolic sine will contribute a residue,

$$a_{r(-1)} = \lim_{s \to \frac{2\pi i r}{\omega_c}} \left[\frac{(s - \frac{2\pi i r}{\omega_c})}{2\sinh(\frac{s\omega_c}{2})} \frac{1}{s} \sqrt{\frac{2m\pi}{|s|}} e^{-s(-mh + \langle\Sigma\rangle - \zeta_n + \frac{V^2 z^2}{\zeta_n - \tilde{E}_f})}\right].$$

Applying L'Hôpital's rule to the first term and simplifying yields:

$$a_{r(-1)} = \frac{(-1)^r}{2\pi i r} \sqrt{\frac{m\omega_c}{|r|}} e^{-\frac{i2\pi r}{\omega_c}(-mh + \langle\Sigma\rangle - \zeta_n + \frac{V^2 z^2}{\zeta_n - \tilde{E}_f})}.$$

We have two integrals to evaluate, the first for the case when n and ω_n are positive and the second for when they are negative. Both paths run along the

imaginary axis (a distance $b \to 0^+$ away), the first from b to $b + i\infty$ and the second from $b - i\infty$ to b. The integrals contain the exponential of the complex variable of integration, s, multiplied by the function $(-mh + \langle\Sigma\rangle - i\omega_n - \mu + \frac{V^2 z^2}{i\omega_n + \mu - \tilde{E}_f})$, whose real part is negative, and whose imaginary part has the opposite sign of ω_n. Thus for the first integral, this exponential will vanish for $|s| \to \infty$ in the upper left plane, and for the second integral, in the lower left plane. So we replace the original contours with the closed contour shown in figure 6.1. The difference in each case is an integral along the real axis, which will not yield an oscillatory term in $1/B$, so we will not include it as part of Ω_{osc}.

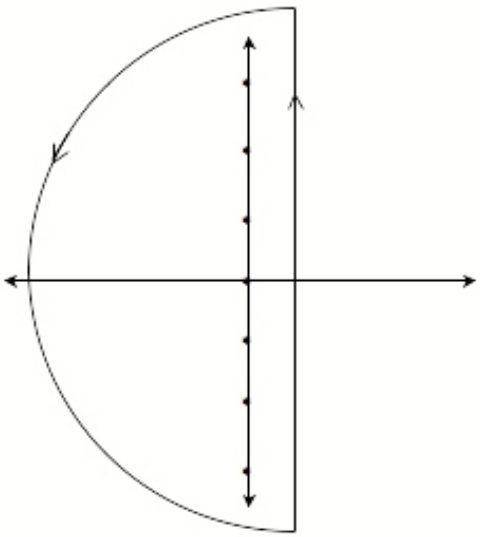

FIGURE 6.1. Contour of integration

With the new contours, the integrals may be evaluated to be $2\pi i$ times the sum of the residues:

$$\Omega = -T\,\frac{L^3 m_b \omega_c}{2\pi h}\sum_{m=-J}^{J} \left[\sum_{n=0}^{\infty} 2\pi i \sum_{r=1}^{\infty} e^{-i\pi/4} a_{r(-1)} - \sum_{n=-\infty}^{0} 2\pi i \sum_{r=1}^{\infty} e^{i\pi/4} a_{-r(-1)}\right]$$

$$= -T\,\frac{L^3 m_b \omega_c}{2\pi h}\sum_{m=-J}^{J} \left[\sum_{n=0}^{\infty}\sum_{r=1}^{\infty} \frac{(-1)^r}{2\pi i r}\sqrt{\frac{m\omega_c}{|r|}} e^{-\frac{i2\pi r}{\omega_c}(-mh+\langle\Sigma\rangle-\zeta_n+\frac{V^2 z^2}{\zeta_n-\tilde{E}_f})}\, e^{-i\pi/4} \right.$$

$$\left. - \sum_{n=-\infty}^{0}\sum_{r=1}^{\infty} \frac{(-1)^r}{-2\pi i r}\sqrt{\frac{m\omega_c}{|-r|}} e^{+\frac{i2\pi r}{\omega_c}(-mh+\langle\Sigma\rangle-\zeta_n+\frac{V^2 z^2}{\zeta_n-\tilde{E}_f})} e^{+i\pi/4}\right].$$

The two terms differ in the sign of the exponential and the sign of n. If we take $n \to -n'$ we can rewrite the second sum so that both sums look the same and can be added directly. When the sign of n changes, the two terms have some parts in common, and other parts which still differ by a sign in the exponential:

$$\Omega = -T\,\frac{L^3 m_b \omega_c}{2\pi h}\sum_{m=-J}^{J}\sum_{n=0}^{\infty}\sum_{r=1}^{\infty} \frac{(-1)^r}{r}\sqrt{\frac{m_b\omega_c}{r}}$$
$$\exp\left(\frac{i2\pi r}{\omega_c}\left(i\omega_n + \frac{i\omega_n V^2 z^2}{\omega_n^2 + (\tilde{E}_f-\mu)^2} - i\Im\langle\Sigma\rangle\right)\right) \times$$
$$\left[\exp\left(\frac{-i2\pi r}{\omega_c}\left(-\mu - mh + \Re\langle\Sigma\rangle - \frac{(\tilde{E}_f-\mu)V^2 z^2}{\omega_n^2+(\tilde{E}_f-\mu)^2}\right) - i\frac{\pi}{4}\right)\right.$$
$$\left. + \exp\left(\frac{+i2\pi r}{\omega_c}\left(-\mu - mh + \Re\langle\Sigma\rangle - \frac{(\tilde{E}_f-\mu)V^2 z^2}{\omega_n^2+(\tilde{E}_f-\mu)^2}\right) + i\frac{\pi}{4}\right)\right].$$

The sum of two exponentials which differ only by the sign of their exponent is a cosine (times two). This cosine is the source of the advertised oscillation in $\Omega_{\rm osc}$. Measuring the f-energy level from the Fermi energy makes the expression slightly more compact, and after some simplification we have:

$$\Omega = -T\,\frac{2L^3 (m_b\omega_c)^{3/2}}{2\pi h}\sum_{m=-J}^{J}\sum_{n=0}^{\infty}\sum_{r=1}^{\infty} \frac{(-1)^r}{r^{3/2}} \times$$
$$\exp\left(\frac{-2\pi r}{\omega_c}\left(\omega_n + \frac{\omega_n V^2 z^2}{\omega_n^2 + (\tilde{E}_f-\mu)^2} - \Im\langle\Sigma\rangle\right)\right) \times$$
$$\cos\left(\frac{2\pi r}{\omega_c}\left(\mu + mh + \frac{(\tilde{E}_f-\mu)V^2 z^2}{\omega_n^2+(\tilde{E}_f-\mu)^2} - \Re\langle\Sigma\rangle\right) - \frac{\pi}{4}\right). \qquad (6.8)$$

The real and imaginary parts of the superconducting self energy are:

$$\Im\left(\Sigma(\mathbf{p},0,\omega_n)\right) = \frac{-1}{\sqrt{\pi}}\frac{\Delta^2\Lambda^2}{v_f^2\sin^2\theta}\int_{-\infty}^{\infty}\frac{dt\, e^{-t^2}\omega_n}{\left(\frac{\Lambda(p^2/2m-\mu)}{v_f\sin\theta}-t\right)^2+\left(\frac{\Lambda}{v_f\sin\theta}\omega_n\right)^2}, \tag{6.9}$$

and

$$\Re\left(\Sigma(\mathbf{p},0,\omega_n)\right) = \frac{1}{\sqrt{\pi}}\frac{\Delta^2\Lambda}{v_f\sin\theta}\int_{-\infty}^{\infty}\frac{dt\, e^{-t^2}\left(-t+\frac{\Lambda(p^2/2m-\mu)}{v_f\sin\theta}\right)}{\left(\frac{\Lambda(p^2/2m-\mu)}{v_f\sin\theta}-t\right)^2+\left(\frac{\Lambda}{v_f\sin\theta}\omega_n\right)^2}. \tag{6.10}$$

However when we take the average over the extremal orbit both these terms simplify, ($k_z = 0$, $\mu = \frac{p^2}{2m}$, $\sin\theta = 1$). The real part vanishes because it is the integral of an odd function over an even interval:

$$\left\langle\Re\left(\Sigma(\mathbf{p},0,\omega_n)\right)\right\rangle_{\text{extremal orbit}} = \frac{\Delta^2\Lambda}{\sqrt{\pi}v_f}\int_{-\infty}^{\infty}\frac{-te^{-t^2}dt}{\left(\frac{\Lambda}{v_f}\omega_n\right)^2+t^2} = 0. \tag{6.11}$$

The imaginary part becomes:

$$\left\langle\Im\left(\Sigma(\mathbf{p},0,\omega_n)\right)\right\rangle_{\text{extremal orbit}} = \frac{-\Delta^2\Lambda^2}{\sqrt{\pi}v_f^2}\omega_n\int_{-\infty}^{\infty}\frac{e^{-t^2}dt}{\left(\frac{\Lambda}{v_f}\omega_n\right)^2+t^2}. \tag{6.12}$$

The integrand here is the product of a Lorentzian multiplied by a Gaussian. Both are peaked at $t = 0$. The value of ω_n determines only how sharp the Lorentzian is. The integral has its largest value at $\omega_n = 0$, however it has only a weak dependence on the value of ω_n. This justifies approximating ω_n by $\omega_o = \frac{\pi}{\beta}$ in all the terms of the sum over n. (Clearly this function is not linear in ω_n, the necessary condition for this term to affect the effective mass.) Further, as this is a low temperature experiment, we'll take the limit $\omega_0 \to 0$. In this limit the Lorentzian becomes a delta function:

$$\lim_{\omega_o\to 0}\frac{\frac{\Lambda}{v_f}\omega_o}{\left(\frac{\Lambda}{v_f}\omega_o\right)^2+t^2} = \pi\delta(t),$$

so

$$\langle \Im\left(\Sigma(\mathbf{p},0,\omega_n)\right)\rangle_{\text{extremal orbit}} = -\sqrt{\pi}\frac{(\Delta(H))^2\Lambda}{v_f}, \tag{6.13}$$

and

$$\begin{aligned}\Omega = -T\,\frac{2L^3(m_b\omega_c)^{3/2}}{2\pi h}\sum_{m=-J}^{J}\sum_{n=0}^{\infty}\sum_{r=1}^{\infty}\frac{(-1)^r}{r^{3/2}}\times \\ \exp\left(\frac{-2\pi r}{\omega_c}\left[\omega_n(1+\frac{V^2z^2}{(T_A-mh)^2})+\sqrt{\pi}\frac{(\Delta(H))^2\Lambda}{v_f}\right]\right)\times \\ \cos\left(\frac{2\pi r}{\omega_c}\left(\mu+mh+\frac{(T_A-mh)V^2z^2}{(T_A-mh)^2}\right)-\frac{\pi}{4}\right).\end{aligned} \tag{6.14}$$

A further simplification will be achieved by the definition of a Kondo temperature, which will be a relevant energy scale. Recall $\tilde{E}_f = E_f + \lambda - mh$. We define $T_A = E_f + \lambda - \mu$ so that $\tilde{E}_f - \mu = T_A - mh$. This term will be large compared to ω_n for low temperatures, so the ω_n's in the denominators of terms in sum over n can safely be ignored. This makes the sum an easy one to do using

$$\sum_{n=0}^{\infty} e^{\alpha(2n+1)} = e^{\alpha}\sum_{n=0}^{\infty}(e^{2\alpha})^n = e^{\alpha}(1-e^{2\alpha})^{-1} = \frac{1}{\sinh\alpha}.$$

Finally we arrive at the result

$$\begin{aligned}\Omega = -k_BT\,\frac{L^3(m_b\hbar\omega_c)^{3/2}}{2\pi^2\hbar^2}\sum_{m=-J}^{J}\sum_{r=1}^{\infty}\frac{(-1)^r}{r^{3/2}}\cos\left(\frac{2\pi r}{\hbar\omega_c}\left(\mu+mh+\frac{V^2z^2}{T_A-mh}\right)-\frac{\pi}{4}\right)\times \\ \exp\left(\frac{-2\pi^{3/2}r}{\omega_c}\frac{(\Delta(H))^2\Lambda}{v_f}\right)\left(\sinh\left[\frac{2r\pi^2k_BT}{\hbar\omega_c}\left(1+\frac{V^2z^2}{(T_A-mh)^2}\right)\right]\right)^{-1},\end{aligned} \tag{6.15}$$

where we note the magnetic field dependence in the order parameter Δ and due to the Zeeman splitting where $h = g_f\mu_BH$ is the reduced magnetic field.

6.2. Results: Effective Mass, Amplitude Reduction

Comparing 6.15 to the canonical Lifshitz-Kosevitch equation 5.1, we see that the hyperbolic sine term has an enhanced mass,

$$m^* \to m_b\left(1+\frac{V^2z^2}{(T_A-mh)^2}\right).$$

This is the field-dependent mass enhancement typical of heavy fermions, first explained by Wasserman and Springford [92]. As shown by Newns and Read [28], self consistency requires

$$V^2 z^2 = \frac{2Dn_f T_A}{N},$$

where $2D$ is the unrenormalized width of the conduction band, n_f the mean number of electrons in the f-level, and $N = 2J+1$ is the degeneracy of the f-level. The mass is smallest and the amplitude of the oscillation largest when the $m = -J$, so the effective mass of the sheet which is most easily observed becomes

$$m^* \to m_b \left(1 + \frac{2Dn_f T_A}{N(T_A + Jg_f \mu_B B)^2}\right).$$

The frequency shift due to the heaviness also reproduces that of Wasserman and Springford. An additional damping factor due to the superconductivity is seen, in accordance with the results of Wasserman and Springford, and Maki. However the superconductivity has no impact on the effective mass, ignoring any changes in Jg_f due to the superconducting state.

6.3. Comparison to Experiment

Nearly all measurements of the de Haas-van Alphen effect in the vortex state of heavy-fermion materials come from the group of Yoshichika Ōnuki at Osaka University in Japan, a group highly regarded for their experimental apparatus and technique. Measurements have been performed with the materials URu_2Si_2 [60], [14], [57]; $CeRu_2$ [59], [58]; UPd_2Al_3 [56], [99], [57]; and $CeCoIn_5$ [63].

Preliminary de Haas-van Alphen measurements in URu_2Si_2 were reported by Bergemann et al. [61], however detailed analysis of the amplitude reduction in the superconducting state does not seem to have been published.

The observation of de Haas-van Alphen becomes more difficult with heavy quasiparticles, and the superconducting state provides additional challenges. Heavy masses reduce the magnitude of the magnetization oscillations, thus higher fields are required to observe them. With fields up to 169 kOersted (17 Tesla), Haga et al. observed oscillations in UPd_2Al_3 due to electrons whose mass is 65 times the bare electron mass. However this is more than four times the upper critical field for this material. These electrons are simply not visible in the mixed state. In addition, there is the additional superconducting damping factor, which significantly reduces the amplitude of oscillations.

The effective mass is determined by plotting the amplitude as a function of temperature. Since the amplitude is a decreasing function of temperature, oscillations due to heavier electrons will quite possibly be visible only in a small range of low temperatures. This could make the interpretation of the masses less certain, since the amplitude is not a linear function of temperature, and must be fit using successive approximations. (The amplitude is multiplied by a function of the effective mass, $1 - \exp(-2m^*\alpha T/H)$, and the slope of this quantity with respect to temperature is the effective mass.) Determination of the exponential damping factors is dependent on knowing the effective mass.

The articles mentioned above uniformly report a reduction in amplitude but no shift in the de Haas-van Alphen freuqencies upon the transition to the superconducting mixed state, as seen in figures 6.2, 6.3, and 6.4 from Haga [56], Hedo [58], and Inada [14]. These figures show the Fourier transform with respect to the inverse magnetic field ($1/H$) of the magnetization, in order to determine the frequency in $1/H$ of the oscillations.

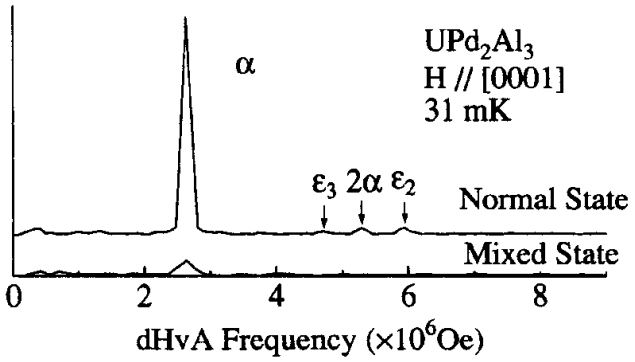

FIGURE 6.2. de Haas-van Alphen oscillations for UPd_2Al_3 from [56].

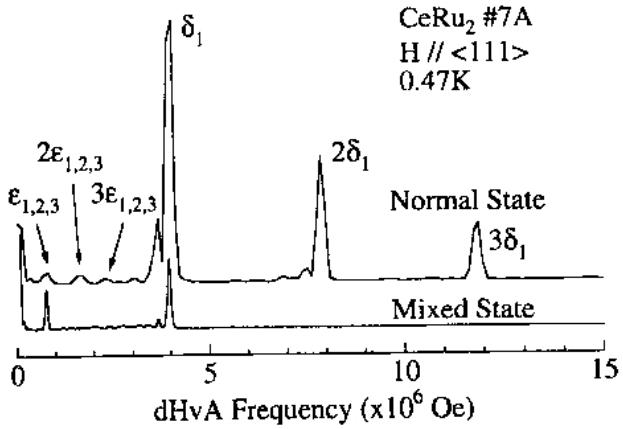

FIGURE 6.3. de Haas-van Alphen oscillations for $CeRu_2$ from [58].

The frequencies are generally in agreement with those predicted by band calculations, although effective masses are not. (The enhanced masses are a many-body effect, not taken into account in a band calculation.)

From the amplitude reduction these authors determine an effective mass (responsible for the temperature-dependent part) and a temperature-independent damping term, called a Dingle factor. The Dingle factor originally referred to the damping due to impurity scattering, parameterized by a Dingle temperature. However in this case the additional amplitude reduction due to the superconducting order

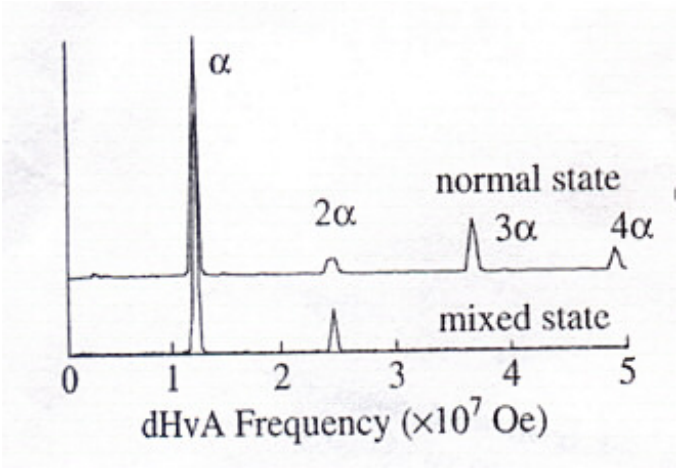

FIGURE 6.4. de Haas-van Alphen oscillations for URu_2Si_2 from [14].

parameter will appear in the Dingle factor, since it is also a temperature-independent term which is exponential in $\frac{1}{B}$. Thus, these authors refer to an additional Dingle temperature in the mixed state. As seen in figures 6.5, 6.6, and 6.7 the Dingle temperature is enhanced in the superconducting state. In each figure the critical field is indicated by a vertical line. At fields below (to the left of) the critical field, the sample is superconducting. At fields above the critical field, the field completely destroys the superconducting state. The authors have fit the field dependence of the Dingle temperature to the theory by Maki, whose result is identical to ours. In the case of UPd_2Al_3 (figure 6.5) the fit using the BCS value for the gap $\frac{2\Delta(0)}{k_b T_c} = 3.54$ is good.

(The peak effect, a rapid increase in the critical current below H_{c2} which may be related to vortex lattice melting, causes hysteresis in magnetization and prevents observation of de Haas-van Alphen oscillaitons in UPd_2Al_3 and $CeRu_2$ at fields slightly below H_{c2}.)

For $CeRu_2$ (figure 6.6) and URu_2Si_2 (figure 6.7), the fit does not have quite the correct field dependence, but the gap sizes obtained from the fit for the different

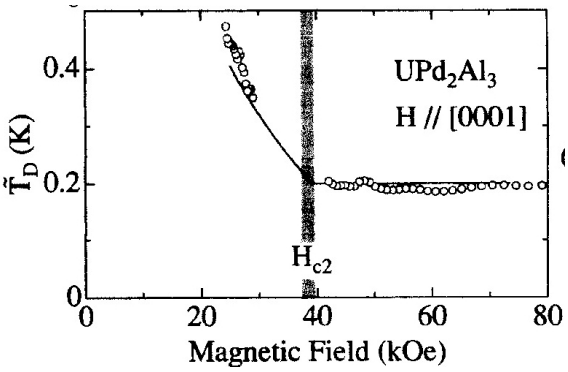

FIGURE 6.5. Dingle temperature vs. field for UPd_2Al_3 from [56].

branches in $CeRu_2$, $\frac{2\Delta}{k_b T_c} = 3.5 - 4.4$, are consistent with those obtained by other methods. In the fit for URu_2Si_2 the BCS value of the gap was used.

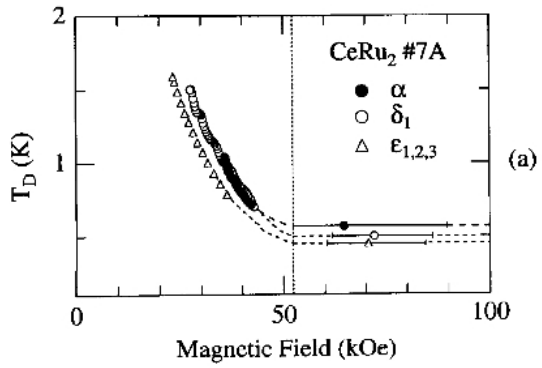

FIGURE 6.6. Dingle temperature vs. field for $CeRu_2$ [58].

However, the effective masses determined for these materials are all reduced noticeably at the transition to the superconducting mixed state.

The authors of these papers note that while Maki's theory gives an expression for the temperature-independent amplitude reduction (additional Dingle temperature), no expression for the mass is given. This is because the only effect of the superconducting self-energy is this additional Dingle temperature. The self-energy term has, to this approximation, no imaginary part and therefore makes no contribu-

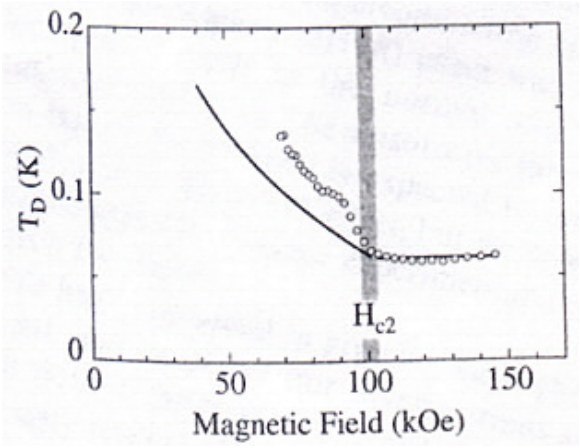

FIGURE 6.7. Dingle temperature vs. field for URu_2Si_2 [14].

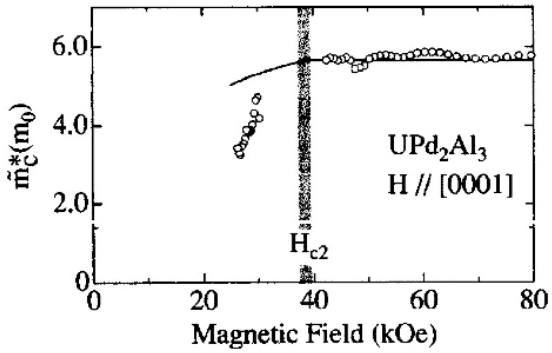

FIGURE 6.8. Effective mass vs. field for UPd_2Al_3 [56].

tion to the effective mass. Nonetheless, these authors have calculated an expression for effective mass from the derivatives of this self-energy on the real axis. This expression is the source of the theoretical curves in two of the plots of effective mass (6.8 and 6.10). This calculation is not appropriate in this case. The ELK theory clearly shows that only a self-energy with an imaginary part may affect the mass, and the particular self-energy which these authors have used in their mass calculation has no imaginary part and causes only the enhanced Dingle temperature. If the effective mass calculated by these authors was correct, one would expect to see a similar mass reduction in all superconductors. However this effect has never

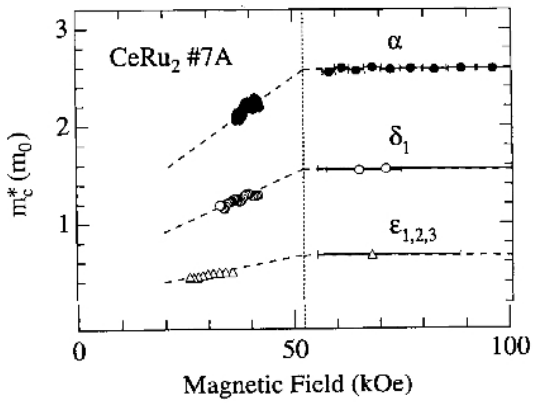

FIGURE 6.9. Effective mass vs. field for $CeRu_2$ [58].

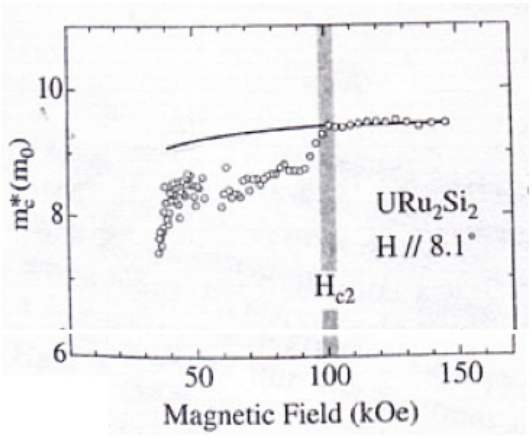

FIGURE 6.10. Effective mass vs. field for URu_2Si_2 [14].

been reported in non-heavy superconductors. The interplay of the heavy-fermion interactions and the superconductivity must be necessary to describe this effect. However, the theory described here also fails to account for it, although it does allow a field-dependent mass common to all heavy-fermion materials.

7. CONCLUSION

The model presented here for heavy-fermion materials in the superconducting state is promising but insufficient. The coexistence of these two many-body effects is likely not treated adequately. One obvious shortcoming which could be remedied is to incorporate superconductivity seperately into each element of the heavy-fermion Green's matrix. As it was done here, the superconducting self-energy affected the energy spectrum of the conduction electrons. However this should not be the only effect if Gorkov's equations were solved using each Green's matrix element. In particular, the mixing Green's functions, G_{fc} and G_{cf} should have a self energy which affects the final outcome. This reflects the fact that the superconductivity arises from the pairing of heavy electrons, and hybridization is a crucial piece of the heaviness. Any model for these materials will have to reflect this reality.

There is some discussion suggesting that multiple order parameters may exist simultaneously in these materials. It would be very interesting to examine the implications of this possibility for the present experimental situation. This might be accomplished by recognizing a second order parameter in addition to the one responsible for conduction-electron pairing. That is in addition to the order parameter

$$\Delta_{c,c} = \langle T_\tau \{\psi_c(\mathbf{r},\tau)\psi_c(\mathbf{r}',\tau')\}\rangle, \tag{7.1}$$

we should include one representing pairing between conduction and localized electrons, i.e.

$$\Delta_{c,f} = \langle T_\tau \{\psi_c(\mathbf{r},\tau)\psi_f(\mathbf{r}',\tau')\}\rangle. \tag{7.2}$$

BIBLIOGRAPHY

7.1. REFERENCES

[1] K. Andres, J.E. Graebner, and H. R. Ott. 4f-virtual-bound-state formation in $CeAl_3$ at low temperatures. *Physical Review Letters*, 35(26):1779–1782, December 1975.

[2] A. C. Hewson. *The Kondo Problem to Heavy Fermions*. Cambridge University Press, Cambridge, 1993.

[3] Neil W. Ashcroft and N. David Mermin. *Solid State Physics*. Saunders College Publishing, Orlando, Florida, 1976.

[4] C Petrovic, P G Pagliuso, M F Hundley, R Movshovich, J L Sarrao, J D Thompson, Z Fisk, and P Monthoux. Heavy-fermion superconductivity in $CeCoIn_5$ at 2.3 K. *Journal of Physics: Condensed Matter*, 13:L337–L342, March 2001.

[5] A D Huxley, C Paulson, O Laborde, J L Tholence, D Sanchez, A Junod, and R Calemczuk. Flux pinning, specific heat and magnetic properties of the Laves phase superconductor $CeRu_2$. *Journal of Physics: Condensed Matter*, 5(41):7709–7718, October 1993.

[6] Masato Hedo, Yoshihiko Inada, Etsuji Yamamoto, Yoshinori Haga, Yoshichika Ōnuki, Yuji Aoki, Tatsuma D. Matsuda, Hideyuki Sato, and Saburo Takahashi. Superconducting properties of $CeRu_2$. *Journal of the Physical Society of Japan*, 67(1):272–279, January 1998.

[7] S.B. Roy. $CeRu_2$ and ZrV_2: Two interesting C15 Laves-phase superconductors. *Philosophical Magazine B*, 65:1435–1444, June 1992.

[8] A. D. Huxley, P. Dalmas de Reotier, A. Yaouanc, D. Caplan, M. Couach P. Lejay, P. C. M. Gubbens, and A. M. Mulders. $CeRu_2$: A magnetic superconductor with extremely small magnetic moments. *Physical Review B*, 54(14):R9666–R9669, October 1996.

[9] C. Geibel, C. Schank, S. Thies, H. Kitazawa, C. D. Bredl, M. Rau A. Böhm, A. Grauel, R. Caspary, R. Helfrich, U. Ahlheim, G. Weber, and F. Steglich. Heavy-fermion superconductivity at T_c =2K in the antiferromagnet UPd_2Al_3. *Zeitschrift für Physik B*, 84(1):1–2, February 1991.

[10] A. Krimmel, P. Fischer, B. Roessli, H. Maletta, C. Geibel, C. Schank, A. Grauel, A. Loidl, and F. Steglich. Neutron diffraction study of the heavy fermion superconductors UM_2Al_3(M=Pd, Ni). *Zeitschrift für Physik B*, 86(2):161–162, June 1992.

[11] C. Geibel, A. Böhn, R. Caspary, K. Gloos, A. Grauel, P. Hellmann, R. Modler, C. Schank, G. Weber, and F. Steglich. Ground state properties of UNi_2Al_3 and UPd_2Al_3. *Physica B*, 186-188:188–194, May 1993.

[12] M.B. Maple, J.W. Chen, Y. Dalichaouch, T. Kohara, C. Rossel, M.S. Torikachvili, M.W. McElfresh, and J.D. Thompson. Partially gapped Fermi surface in the heavy-electron superconductor URu_2Si_2. *Physical Review Letters*, 56(2):185–188, January 1986.

[13] C. Broholm, J.K. Kjems, W.J.L. Buyers, P. Matthews, T.T.M. Palstra, A.A. Menovsky, and J.A. Mydosh. Magnetic excitations and ordering in the heavy-electron superconductor URu_2Si_2. *Physical Review Letters*, 58(14):1467–1470, April 1987.

[14] Y. Inada, H. Ohkuni, M. Hedo, Y. Tokiwa, K. Sakurai, Y. Haga, E. Yamamoto, T. Honma, and Y.Ōnuki. de Haas-van Alphen effect of the heavy-fermion superconductor URu_2Si_2. *Physica B*, 259-261:642–643, January 1999.

[15] P.W. Anderson. Localized magnetic states in metals. *Physical Review*, 124:41–53, October 1961.

[16] Claude Cohen-Tannoudji, Bernard Diu, and Franck Laloë. *Quantum Mechanics, Volume I.* John Wiley and Sons, New York, 1977.

[17] Claude Cohen-Tannoudji, Bernard Diu, and Franck Laloë. *Quantum Mechanics, Volume II.* John Wiley and Sons, New York, 1977.

[18] P.A. Lee, T.M. Rice, J.W. Serene, L.J. Sham, and J.W. Wilkins. Theories of heavy-electron systems. *Comments in Condensed Matter Physics*, 12(3):99–161, 1986.

[19] Peter Fulde. Introduction to the theory of heavy fermions. *Journal of Physics F: Metallic Physics*, 18:601–639, 1988.

[20] P.B. Wiegmann. Towards an exact solution of the Anderson model. *Physics Letters A*, 80(2-3):163–167, November 1980.

[21] Norio Kawakami and Ayao Okiji. Exact expression of the ground-state energy for the symmetric Anderson model. *Physics Letters A*, 86(9):483–486, December 1981.

[22] J. W. Rasul and A. C. Hewson. Bethe ansatz and 1/N expansion results for N-fold degenerate magnetic impurity models. *Journal of Physics C (Solid State Physics)*, 17(14):2555–2573, May 1984.

[23] Piers Coleman. New approach to the mixed-valence problem. *Physical Review B*, 29(6):3035–3044, March 1984.

[24] S.E. Barnes. New method for the Anderson model. *Journal of Physics F: Metallic Physics*, 6(7):1375–1383, July 1976.

[25] A. A. Abrikosov. *Physics (NY)*, 1(2), 1965.

[26] N. Read and D.M. Newns. On the solution of the Coqblin-Schreiffer Hamiltonian by the large-N expansion technique. *Journal of Physics C: Solid State Physics*, 16(17):3273–3295, June 1983.

[27] N. Read and D.M. Newns. A new functional integral formalism for the degenerate Anderson model. *Journal of Physics C: Solid State Physics*, 16(29):L1055–L1060, October 1983.

[28] D.M. Newns and N. Read. Mean field theory of intermediate valence/heavy fermion systems. *Advances in Physics*, 36(6):799–849, 1987.

[29] A.A. Abrikosov, L.P. Gorkov, and I.E. Dzyaloshinski. *Methods of Quantum Field Theory in Statistical Physics*. Dover Publications, New York, 1963, 1975.

[30] Gerald D. Mahan. *Many Particle Physics*. Springer, New York, 2000.

[31] Alexander L. Fetter and John Dirk Walecka. *Quantum Theory of Many Particle Systems*. Mcgraw-Hill College, New York, 1971.

[32] A. A. Abrikosov. On the magnetic properties of superconductors of the second group. *Soviet Physics JETP*, 5(6):1174–1182, December 1957.

[33] U. Brandt, W. Pesch, and L. Tewordt. Theory of the density of states of pure type-II superconductors in high magnetic fields. *Zeitschrift für Physik*, 201:209–221, 1967.

[34] J. Bardeen, L. N. Cooper, and J. R. Schrieffer. Theory of superconductivity. *Physical Review*, 108(5):1175–1204, December 1957.

[35] H Won, S Haas, D Parker, S Telang, A Vanyolos, and K Maki. BCS theory of nodal superconductors. xxx.arxiv.org/abs/cond-mat/0501463, 2005.

[36] P. M. Oppeneer and G. Varelogiannis. Efficient self-consistent calculations of multiband superconductivity in UPd_2Al_3. *Physical Review B*, 68(21):214512, 2003.

[37] Grzegorz Haran and A D S Nagi. Weak anisotropic impurity scattering in unconventional superconductors. *Solid State Communications*, 101:71, 1997.

[38] Andrew Peter Mackenzie and Yoshiteru Maeno. The superconductivity of Sr_2RuO_4 and the physics of spin-triplet pairing. *Reviews of Modern Physics*, 75(2):657–712, May 2003.

[39] Robert Joynt and Louis Taillefer. The superconducting phases of UPt_3. *Reviews of Modern Physics*, 74(1):235–294, January 2002.

[40] W.N. Hardy, D.A. Bonn, D.C. Morgan, Ruixing Liang, and Kuan Zhang. Precision measurements of the temperature dependence of λ in $YBa_2Cu_3O_6.95$: Strong evidence for nodes in the gap function. *Physical Review Letters*, 70(25):3999–4002, June 1993.

[41] T. Watanabe, K. Izawa, Y. Kasahara, Y. Haga, Y. Ōnuki, P. Thalmeier, K. Maki, and Y. Matsuda. Superconducting gap function in antiferromagnetic heavy-fermion UPd_2Al_3 probed by angle-resolved magnetothermal transport measurements. *Physical Review B*, 70(18):184502–184510, November 2004.

[42] J.P. Brison, L. Glémot, H. Suderow, A., S. Kambe, and J. Flouquet. Heavy fermion superconductivity. *Physica B*, 280(1-4):165–171, May 2000.

[43] G.E. Volovik. Superconductivity with lines of gap nodes: density of states in the vortex. *JETP Letters*, 58(5-6):469–473, September 1993.

[44] L Tewordt and D Fay. Thermal conductivity near H_{c2} for spin-triplet superconducting states with line nodes in Sr_2RuO_4. *Physical Review B*, 64:024528, 2001.

[45] L Tewordt and D Fay. Thermal conductivity in the vortex state of the superconductor UPd_2Al_3. *Physical Review B*, 72:014502, 2005.

[46] H Won, D Parker, K Maki, T Watanabe, and K Izawa Y Matsuda. Gap symmetry of superconductivity in UPd_2Al_3. xxx.arxiv.org/abs/cond-mat/0407271, 2004.

[47] H. R. Ott, H. Rudigier, Z. Fisk, and J.L. Smith. UBe_{13}: An unconventional actinide superconductor. *Physical Review Letters*, 50(20):1595–1598, May 1983.

[48] R. A. Fisher, S. Kim, B. F. Woodfield, N. E. Phillips, L. Taillefer, K. Hasselbach, J. Flouquet, A. L. Giorgi, and J. L. Smith. Efficient self-consistent calculations of multiband superconductivity in UPd_2Al_3. *Physical Review Letters*, 62(12):1411–1414, March 1989.

[49] A Sulpice, P. Gandit, J. Caussy, J. Fouquet, D. Jaccard, P. Lejay, and J. L. Tholence. Thermodynamic and transport properties of UPt_3. *Journal of Low Temperature Physics*, 62(1-2):39–54, January 1986.

[50] B. S. Shivaram, Y. H. Jeong, T. F. Rosenbaum, and D. G. Hinks. Anisotropy of transverse sound in the heavy-fermion superconductor UPt_3. *Physical Review Letters*, 56(10):1078–1081, March 1986.

[51] Y. Kohori, H. Shibai, T. Kohara, Y. Oda, Y. Kitaoka, and K. Asayama. ^{195}Pt NMR study of the heavy-fermion superconductor UPt_3. *Journal of Magnetism and Magnetic Materials*, 76-77:478–480, 1988.

[52] C. Broholm, G. Aeppli, R. N. Kleiman, D. R. Harshman, D. J. Bishop, E. Bucher, D. Ll. Williams, E. J. Ansaldo, and R. H. Heffner. Anisotropic temperature dependence of the magnetic-field penetration in superconducting UPt_3. *Physical Review Letters*, 65(15):2062–2065, October 1990.

[53] H. Tou, Y. Kitaoka, K. Asayama, N. Kimura, Y. Ōnuki, E. Yamamoto, and K. Maezawa. Odd-parity superconductivity with parallel spin pairing in UPt_3: Evidence from ^{195}Pt knight shift study. *Physical Review Letters*, 77(7):1374–1377, August 1996.

[54] H. Tou, Y. Kitaoka, K. Ishida, K. Asayama, N. Kimura, Y. Ōnuki, E. Yamamoto, Y. Haga, and K. Maezawa. Nonunitary spin-triplet superconductivity in UPt_3: Evidence from ^{195}Pt knight shift study. *Physical Review Letters*, 80(14):3129–3132, April 1998.

[55] Hideki Tou, Kenji Ishida, and Yoshio Kitaoka. Quasiparticle spin susceptibility in heavy-fermion superconductors : An NMR study compared with specific heat results. *Journal of the Physical Society of Japan*, 74:1245, 2005.

[56] Yoshinori Haga, Yoshihiko Inada, Kenji Sakurai, Yoshihumi Tokiwa, Etsuji Yamamoto, Tetsuo Honma, and Yoshichika Ōnuki. De Haas-van Alphen oscillation in both the normal and superconducting mixed states of UPd_2Al_3. *Journal of the Physical Society of Japan*, 68(2):342–345, February 1999.

[57] Y. Inada andH. Ohkuni, Y. Haga, Y. Tokiwa, K. Sakurai, T. Honma, E. Yamamoto, and Y.Ōnuki. Anisotropic superconducting energy gap studied by the dHvA effect in URu_2Si_2 and UPd_2Al_3. *Physica B*, 281-282:996–997, June 2000.

[58] Hedo M., Inada Y., Sakurai K., Yamamoto E., Haga Y., Ōnuki Y., Takahashi S., Higuchi M., Maehira T., and Hasegawa A. Magnetoresistance and de Haas-van Alphen oscillation in normal and superconducting $CeRu_2$. *Philosophical Magazine B*, 77(4):975–1000, April 1998.

[59] Y. Inada, M. Hedo, T. Ishida, E. Yamamoto, Y. Haga, and Y.Ōnuki. dHvA oscillation in the superconducting mixed state of $CeRu_2$. *Physica B*, 230-232:387–390, February 1997.

[60] Hitoshi Ohkuni, Takashi Ishida, Yoshihiko Inada, Yoshinori Haga, Etsuji Yamamoto, Yoshichika Ōnuki, and Saburo Takahashi. De Haas-van Alphen oscillation in the superconducting mixed state of URu_2Si_2. *Journal of the Physical Society of Japan*, 66(4):945–948, April 1997.

[61] C. Bergemann, S. R. Julian, G. J. McMullan, B. K. Howard, G. G. Lonzarich, P. Lejay, J. P. Brison, and J. Flouquet. Quantum oscillations in URu_2Si_2. *Physica B*, 230-232:348–350, February 1997.

[62] Yoshichika Imagenuki, Yoshihiko Inada, Hitoshi Ohkuni, Rikio Settai, Noriaki Kimura, Haruyoshi Aoki, Yoshinori Haga, and Etuji Yamamoto. Itinerant f-electron systems of cerium and uranium compounds. *Physica B*, 280(1-4):276–280, May 2000.

[63] R Settai, H Shishido, S Ikeda, Y Murakawa, M Nakashima, D Aoki1, Y Haga, H Harima, and Y Ōnuki. Quasi-two-dimensional fermi surfaces and the de Haas-van Alphen oscillation in both the normal and superconducting mixed states of $CeCoIn_5$. *Journal of Physics: Condensed Matter*, 13:L627–L634, July 2001.

[64] Y. He, C. Muirhead, A. Bradshaw, J. Abell, C. Schank, G. Geibel, and F. Steglich. Coherence of the superconducting wavefunction between the heavy-fermion superconductor UPd_2Al_3 and niobium. *Nature*, 357(6375):227–230, May 1992.

[65] R. Feyerherm, A. Amato, F. N. Gygax, A. Schenck, C. Geibel, F. Steglich, N. Sato, and T. Komatsubara. Coexistence of local moment magnetism and heavy-fermion superconductivity in UPd_2Al_3. *Physical Review Letters*, 73(13):1849–1852, September 1994.

[66] Hideki Tou, Yoshio Kitaoka, Kunisuke Asayama, Christoph Geibel, Christina Schank, and Frank Steglich. d-wave superconductivity in antiferromagnetic heavy-fermion compound UPd_2Al_3—evidence from ^{27}Al NMR/NQR studies. *Journal of the Physical Society of Japan*, 64(3):725–729, March 1995.

[67] R. Caspary, P. Hellmann, M. Keller, G. Sparn, C. Wassilew, R. Köhler, C. Geibel, C. Schank, F. Steglich, and N. E. Phillips. Unusual ground-state properties of UPd_2Al_3: Implications for the coexistence of heavy-fermion superconductivity and local-moment antiferromagnetism. *Physical Review Letters*, 71(13):2146–2149, September 1993.

[68] Masahiko Hiroi, Masafumi Sera, Norio Kobayashi, Yoshinori Haga, Etsuji Yamamoto, and Yoshichika Ōnuki. Thermal conductivity of a heavy fermion superconductor UPd_2Al_3 single crystal. *Journal of the Physical Society of Japan*, 66(6):1595–1598, June 1997.

[69] M. Jourdan, M. Huth, and H. Adrian. Superconductivity mediated by spin fluctuations in the heavy-fermion compound UPd_2Al_3. *Nature*, 398(6722):47–49, March 1999.

[70] N. Bernhoeft, N. Sato, B. Roessli, N. Aso, A. Hiess, G. H. Lander, Y. Endoh, and T. Komatsubara. Enhancement of magnetic fluctuations on passing be-

low T_c in the heavy fermion superconductor UPd_2Al_3. *Physical Review Letters*, 81(19):4244 – 4247, November 1998.

[71] P Thalmeier, T Watanabe, K Izawa, and Y Matsuda. Field-angle resolved specific heat and thermal conductivity in the vortex phase of UPd_2Al_3. xxx.arxiv.org/abs/cond-mat/0501103, 2005.

[72] Kazumi Maki, Stephan Haas, David Parker, and Hyekyung Won. Perspectives on nodal superconductors. xxx.arxiv.org/abs/cond-mat/0407269, 2004.

[73] C. Broholm, H. Lin, P. T. Matthews, T. E. Mason, W. J. L. Buyers, M. F. Collins, A. A. Menovsky, J. A. Mydosh, and J. K. Kjems. Magnetic excitations in the heavy-fermion superconductor URu_2Si_2. *Physical Review B*, 43(16):12809–12822, June 1991.

[74] A Virosztek, K Maki, and B Dora. Micromagnetism in URu_2Si_2 and high temperature superconductors. *International Journal of Modern Physics B*, 16:1667, 2002.

[75] J. P. Brison, N. Keller, P. Lejay, A. Huxley, L. Schmidt, A. Buzdin, N. R. Bernhoeft, I. Mineev, A. N. Stepanov, J. Flouquet, D. Jaccard, S. R. Julian, and G. G. Lonzarich. Very low temperature properties of heavy fermion materials. *Physica B*, 199 - 200:70–75, April 1994.

[76] Kazuyuki Matsuda, Yoh Kohori, and Takao Kohara. Existence of line nodes in the superconducting energy gap of antiferromagnetic superconductor URu_2Si_2—^{101}Ru NQR study. *Journal of the Physical Society of Japan*, 65(3):679–682, March 1996.

[77] Stephan Haas, Kazumi Maki, Thomas Dahm, and Peter Thalmeier. Anatomy of gossamer superconductivity. xxx.arxiv.org/abs/cond-mat/0311537, 2003.

[78] R B Laughlin. Gossamer Superconductivity. xxx.arxiv.org/abs/cond-mat/0209269, 2002.

[79] J. G. Sereni, G. L. Nieva, G. Schmerber, and J. P. Kappler. Evidences for unconventional superconductivity in rare-earth intermetallics. *Modern Physics Letters B*, 3(16):1225–1231, November 1989.

[80] Kazuyuki Matsuda, Yoh Kohori, and Takao Kohara. 101Ru NQR study in $CeRu_2$. *Physica B*, 223-224:166–168, June 1996.

[81] A V Moskalenko, Yu G Naidyuk, I K Yanson, M Hedo, Y Inada, Y Ō, Y Haga, and E Yamamoto. Superconducting gap and pair breaking in $ceru_2$ studied by point contacts. *Fizika Nizkikh Temperatur*, 27:831, 2001.

[82] Hideaki Sakata, Nobuhiko Nishida, Masato Hedo, Kenji Sakurai, Yoshihiko Inada, Yoshichika Ō, Etsuji Yamamoto, and Yoshinori Haga. Vortex lattice and

quasiparticle density of states in $CeRu_2$ studied by scanning tunneling spectroscopy. *Journal of the Physical Society of Japan*, 69(7):1970–1973, July 2000.

[83] T. Ekino, H. Fujii, T. Nakama, and K. Yagasaki. Electron tunneling into superconducting $CeRu_2$. *Soviet Physics JETP*, 56(13):78517854, October 1997.

[84] N. K. Sato, N. Aso, K. Miyake, R. Shiina, P. Thalmeier, G. Varelogiannis, C. Geibel, F. Steglich, P. Fulde, and T. Komatsubara. Strong coupling between local moments and superconducting 'heavy' electrons in UPd_2Al_3. *Nature*, 410(6826):340–343, March 2001.

[85] N.D.Mathur, F. M. Grosche, S. R. Julian, I. R. Walker, D. M. Freye, R. K. W. Haselwimmer, and G. G. Lonzarich. Magnetically mediated superconductivity in heavy fermion compounds. *Nature*, 394(6688):39–43, 2 July 1998.

[86] Toru Moriya and Kazuo Ueda. Spin fluctuations and high temperature superconductivity. *Advances in Physics*, 49(5):555–606, July 2001.

[87] Toru Moriya and Kazuo Ueda. Antiferromagnetic spin fluctuation and superconductivity. *Reports on Progress in Physics*, 66(8):1299–1341, August 2003.

[88] Andrey V Chubukov, David Pines, and Joerg Schmalian. A spin fluctuation model for d-wave superconductivity. xxx.arxiv.org/abs/cond-mat/0201140, 2002.

[89] Eugene Demler, Werner Hanke, and Shou-Cheng Zhang. SO(5) theory of antiferromagnetism and superconductivity. *Reviews of Modern Physics*, 76(6):909–974, July 2004.

[90] E. Helfand and N. R. Werthamer. Temperature and purity dependence of the superconducting critical field, H_{c2}. *Physical Review Letters*, 13(23):686–688, December 1964.

[91] L. A. Linden Levy and A. Wasserman. The influence of the crystal potential on the de Haas-van Alphen effect. Undergraduate Thesis, Oregon State University Department of Physics, 2001.

[92] A. Wasserman and M. Springford. The influence of many-body interactions on the de Haas-van Alphen effect. *Advances in Physics*, 45(6):471–503, November 1996.

[93] Eilenberger. *Zeitschrift für Physik*, 190:142, 1966.

[94] de Haas and van Alphen. *Proceedings of the Netherlands Royal Academy of Science*, 33:680, 1930.

[95] L. Landau. *Zeitschrift für Physik*, 64:629, 1930.

[96] Lifshitz and Kosevitch. *Soviet Physics JETP*, 2:636, 1956.

[97] Kazumi Maki. Quantum oscillation in vortex states of type-II superconductors. *Physical Review B*, 1991(6):2861–2862, August 44.

[98] J. W. Rasul. De Haas-van Alphen effect in the Anderson lattice for large orbital degeneracy. *Physical Review B*, 39(1):663–670, January 1989.

[99] Y. Haga, Y. Inada, H. Yamagami, K. Sakurai, Y. Tokiwa, E. Yamamoto, T. Honma, and Y.Ōnuki. Observation of heavy electrons in UPd_2Al_3. *Physica B*, 281-282:780–781, June 2000.